JOURNAL OF GEOPHYSICAL RESEARCH, VOL. 106, NO. E11, PAGES 27,865–27,885, NOVEMBER 25, 2001

Interior of the Moon: The presence of garnet in the primitive deep lunar mantle

Clive R. Neal

Department of Civil Engineering and Geological Sciences, University of Notre Dame, Notre Dame, Indiana

Abstract. New trace element data have been generated by inductively coupled plasma-mass spectrometry (ICP-MS) for 65 high- and low-Ti mare basalts from the Apollo 11, 12, 14, 15, and 17 landing sites. These data demonstrate that ratios of the high field strength elements and yttrium are generally chondritic in the mare source regions for the low-Ti basalts but nonchondritic in the high-Ti basalts and potassium, rare earth elements, and phosphorus (KREEP); such differences can be explained by addition and subtraction (respectively) of ilmenite. This interpretation is consistent with derivation of the basalts from lunar magma ocean (LMO) cumulates through which late stage ilmenite has sunk and mixed with earlier magma ocean products. Compositional differences between the mare basalts and volcanic glass beads suggest that at least some of the latter were derived from a garnet-bearing source region. Siderophile and chalcophile element data suggest that the garnet-bearing source escaped the LMO melting event and thus represents primitive Moon material. The remaining glasses are generally very low Ti (VLT) and appear to have been derived from early LMO cumulates (i.e., olivine and orthopyroxene, similar to the VLT basalts). The remaining glasses were derived from below the LMO cumulates, and as the magmas rose they underwent sequential assimilation (to varying degrees) initially of an ilmenite-rich cumulate followed by a KREEP component. This study presents geochemical evidence for the existence of garnet in a mare source and demonstrates the likelihood that the LMO was not "whole Moon," thus preserving primitive lunar material, which has acted as the source region for at least some of the volcanic glasses.

1. Introduction

Since the return of the first lunar samples, there have been numerous models formulated for lunar evolution and the development of the mare source regions. It is outside the scope of this paper to review all of these models, but a brief summary is given here.

Lunar research has highlighted the formation of Earth's only natural satellite via collision between a Mars-sized planetesimal and an already differentiated Earth [*Hartmann and Davis*, 1975; *Hartmann*, 1986; *Cameron and Ward*, 1976; *Cameron*, 1986; *Cameron and Benz*, 1991; *Cameron and Canup*, 1998] on the basis of angular momentum, Earth:Moon mass ratio, and lunar orbit (see *Taylor* [1982 and 1990] for review). Material ejected from this collision coalesced and the heat generated during formation triggered a melting event, creating the lunar magma ocean (LMO) [e.g., *Smith et al.*, 1970; *Wood et al.*, 1970; *Warren and Wasson*, 1979; *Taylor*, 1982; *Warren*, 1985]. Cooling of this magma ocean produced layered igneous cumulates that, in the simplest of models, resulted in olivine and pyroxene forming the source regions for mare magmatism and the lighter plagioclase forming the lunar crust [e.g., *Taylor and Jâkes*, 1974; *Warren*, 1985]. More complicated models demonstrated that late stage ilmenite-rich (dense) cumu-lates would be unstable and may sink [e.g., *Kesson and Ringwood*, 1976; *Ringwood and Kesson*, 1976], producing limited mixing of the cumulate layers [*Snyder et al.*, 1992] or full-scale overturn of the cumulate pile [e.g., *Hughes et al.*, 1988, 1989; *Spera*, 1992; *Hess*, 1993, 1994; *Hess and Parmentier*, 1995]. The scale of the lunar magma ocean has been debated: was this whole-moon melting [cf. *Hess*, 1993, 1994; *Hess and Parmentier*, 1995] or only the outer ~400-500 km [cf. *Warren*, 1985]? If whole-moon melting is invoked, then differentiation of the Moon into a flotation plagioclase-rich crust, a mafic mineral cumulate mantle, and a Fe-rich core is more easily facilitated. However, as pointed out by *Hess and Parmentier* [1995], if the material that formed the Moon came primarily from the already differentiated Earth mantle, then there may not be enough iron to form a metallic Fe core. These authors suggested that the lunar core is made up of the dense, ilmenite-rich, late stage cumulates from the LMO.

Lunar volcanism, whether as volcanic glass beads or as basalts, allows the nature of the magmatic source regions to be examined through geochemistry and experimental petrology. With the possible exception of Apollo 17 very low titanium (VLT) glasses, none of the glasses are parental to the mare basalts at the specific landing sites [e.g., *Longhi*, 1987, 1990, 1992; *Delano*, 1990; *Shearer et al.*, 1991]. Although many attempts have been made to link the crystalline basalts with the volcanic glasses [e.g., *Vaniman and Papike*, 1977; *Taylor et al.*, 1978], no connection has been unequivocally established, and petrogenetic relationships between mare basalts and volcanic glasses remain only grossly defined in terms of similar igneous processes.

Experimental studies on the volcanic glasses indicate derivation from pressures in the region of 18-25 kbar (360-520 km), which may be below the cumulate lunar mantle formed by magma ocean crystallization [e.g., *Shirley and Wasson*, 1981; *Delano*, 1986; *Longhi*, 1992, 1993]. *Longhi* [1992] reported the pressures of multiple saturation for primitive mare basalts to be between 5

Paper number 2000JE001386.
0148-0227/01/2000JE001386$09.00

and 12.5 kbar (100-250 km). Even though multiple saturation pressures and temperatures of the basalts may have been conducted on evolved (i.e., nonprimary) compositions, thus yielding a minimum depth, volatile contents and isotope ratios demonstrate the derivation of the mare basalts and volcanic glasses from compositionally distinct and separate sources [e.g., *Tatsumoto et al.*, 1973, 1987].

Twenty-five distinct groups of volcanic glasses have been defined from existing lunar sample collections, 12 of which are very low Ti and picritic [*Delano and Livi*, 1981; *Delano*, 1986]. A model proposed by *Hubbard and Minear* [1976] and revived by *Wagner and Grove* [1993, 1995, 1997] and *Elkins et al.* [2000] required that the parental magma(s) of the volcanic glass beads was/were derived from primitive (undifferentiated by the LMO event) lunar mantle, and it/they assimilated (to varying degrees) late stage, ilmenite-rich LMO cumulates. This model accounts for the wide range of TiO_2 contents of the volcanic glasses (<1 wt% to >16 wt%) and the fact that the glasses appear to be undersaturated with respect to ilmenite [e.g., *Green et al.*, 1975; *Longhi*, 1992, 1993; *Hess*, 1993]. Conversely, *Shearer et al.* [1996a] argued against assimilation of ilmenite-rich cumulates on the basis of Zr, Nb, and Ce abundances and ratios in the volcanic glasses. They argued that increasing Zr and Nb contents were the result of variable potassium, rare earth elements, and phosphorus (KREEP) components in the source regions. *Shearer et al.* [1991] concluded that the primitive members of each of the 25 glass groups were composed of both primitive and evolved cumulate components, whereas *Galbreath et al.* [1990] concluded that three cumulate components (a differentiated cumulate, trapped residual liquid, and extremely Fe-rich components) were required. If this is the case, then the magmas that formed the volcanic glasses do not represent a single source, but rather a mixture, and any source modeling will yield results consistent with (1) catastrophic/limited overturn of the cumulate pile [e.g., *Spera*, 1992] or (2) polybaric melting models [e.g., *Longhi*, 1992] and (3) assimilation models [e.g., *Wagner and Grove*, 1997; *Elkins et al.*, 2000]. *Hughes et al.* [1988, 1989] interpreted the volcanic glasses as being products of the cumulate lunar mantle that experienced catastrophic overturn. In contrast, *Hess* [1993] demonstrated that the major element concentrations could not be modeled using this approach as well as arguing that assimilation models required an unreasonably high ilmenite/diopside ratio. He concluded that volcanic glasses ranging from 4.6 to 13.5 wt% TiO_2 were derived from depths of 400-500 km, leaving an olivine + orthopyroxene residuum [cf. *Green et al.*, 1975; *Kesson*, 1975; *Walker et al.*, 1975].

Using multiple saturation experiments as a guide, it appears that the mare basalts originated at shallower depths than the volcanic glasses and within the region of "cumulate" mantle formed by LMO crystallization [cf. *Taylor*, 1982]. Analyzing mare basalts with a view to identifying source compositions is fraught with difficulties, not least of which is obtaining a representative analysis of a given mare basalt sample [e.g., *Haskin et al.*, 1977; *Lindstrom and Haskin*, 1981; *Schuraytz and Ryder*, 1988, 1991]. As with the volcanic glasses, understanding post-magma-generation evolutionary processes is critical before attempting any source modeling. Processes such as crystal fractionation and accumulation are very prevalent in the crystalline mare basalts [e.g., *Warner et al.*, 1979, 1980; *James and Wright*, 1972; *Walker et al.*, 1976; *Dungan and Brown*, 1977; *Vetter et al.*, 1988; *Neal et al.*, 1990, 1994], and combined assimilation and fractional crystallization (AFC) processes were important in the generation of the Apollo 14 high-alumina and very high potassium (VHK) mare basalts [*Shervais et al.*, 1985a, 1985b; *Neal et al.*, 1988a, 1988b, 1989].

In summary, the Moon appears to have experienced a magma ocean event that produced mafic cumulates. Overturn of the cumulate pile to some extent is required to account for a pervasive negative Eu anomaly in the mare basalts and volcanic glasses, presumably resulting from the extraction of the anorthositic crust. Early cumulates would not include plagioclase and so would exhibit no negative Eu anomaly (assuming a starting material with a chondritic REE profile). However, did the magma ocean involve whole-moon melting? If not, what depth did the melting event reach? The purpose of this paper is to use the compositions of the mare volcanic products (crystalline basalts and glass beads) to investigate the interior of the Moon to evaluate the nature of the magmatic source regions terms of the lunar magma ocean model. This paper investigates whole-moon and partial-moon melting and presents results of an initial study of mare basalts that uses trace element data generated by inductively coupled plasma-mass spectrometry (ICP-MS).

2. Limitations of the Current Data Set

Using mare basalt and volcanic glass data to look at source compositions is problematical because of inconsistency in and scarcity of data. For example, literature values for the Apollo 12 suite report data obtained from aliquots of different sizes and using different analytical techniques. Niobium and Zr are usually reported from X-ray fluorescence (XRF) analyses, and Ta and Hf are usually reported from instrumental neutron activation (INA) analyses. This has produced a wide range of Nb/Ta and Zr/Hf ratios (e.g., Figure 1), which has in turn generated confusion when these elements are used to delineate mare source regions. As the volcanic glass beads are so small, trace element data were difficult to obtain (but see *Hughes et al.* [1988, 1989]) until the advent of the ion microprobe [e.g., *Galbreath et al.*, 1990; *Shearer et al.*, 1989, 1990, 1991, 1994, 1996a, 1996b]. Even here, the high field strength element (HFSE) determinations are generally restricted to Zr.

The majority of published work concentrating on the HFSEs has highlighted Zr-Hf ratios of mare basalts although literature data can give very different values for the same basalt (Figure 1). For example, *Duncan et al.* [1974] used Zr-Y-Nb correlations to conclude that Apollo 17 basaltic liquids were derived by melting of a preexisting cumulate in which ilmenite and a Zr-Y-Nb-rich phase or phases were cumulus minerals. Interpretations could be fundamentally flawed because of inconsistencies in the database, such as those defined in Figure 1. However, several studies have produced HFSE data from the same sample aliquot. *Chyi and Ehmann* [1973], *Ehmann et al.* [1975], and *Garg and Ehmann* [1976] reported Zr/Hf ratios in lunar materials ranging from <25 to >50 with KREEP possessing high Zr/Hf ratios. It was concluded that the Zr-Hf fractionation apparent in lunar samples was due to the reduction of Zr^{4+} to Zr^{3+} while Hf remained in the tetravalent state. *Hughes and Schmitt* [1985] used Zr-Hf-Ta data derived by high-precision coincidence instrumental neutron activation on the same sample to define a mean Zr/Hf for KREEP of 41.0 ± 0.4, ~39 for Apollo 15 basalts, and 30-32 for Apollo 11, 12, and 17 basalts, with the decreases in Zr/Hf broadly correlating with La/Yb. Ta/Hf ratios are higher for Apollo 11 and 17 basalts relative to those from other sites. *Hughes and Schmitt* [1985] concluded that either ilmenite and armalcolite fractionated

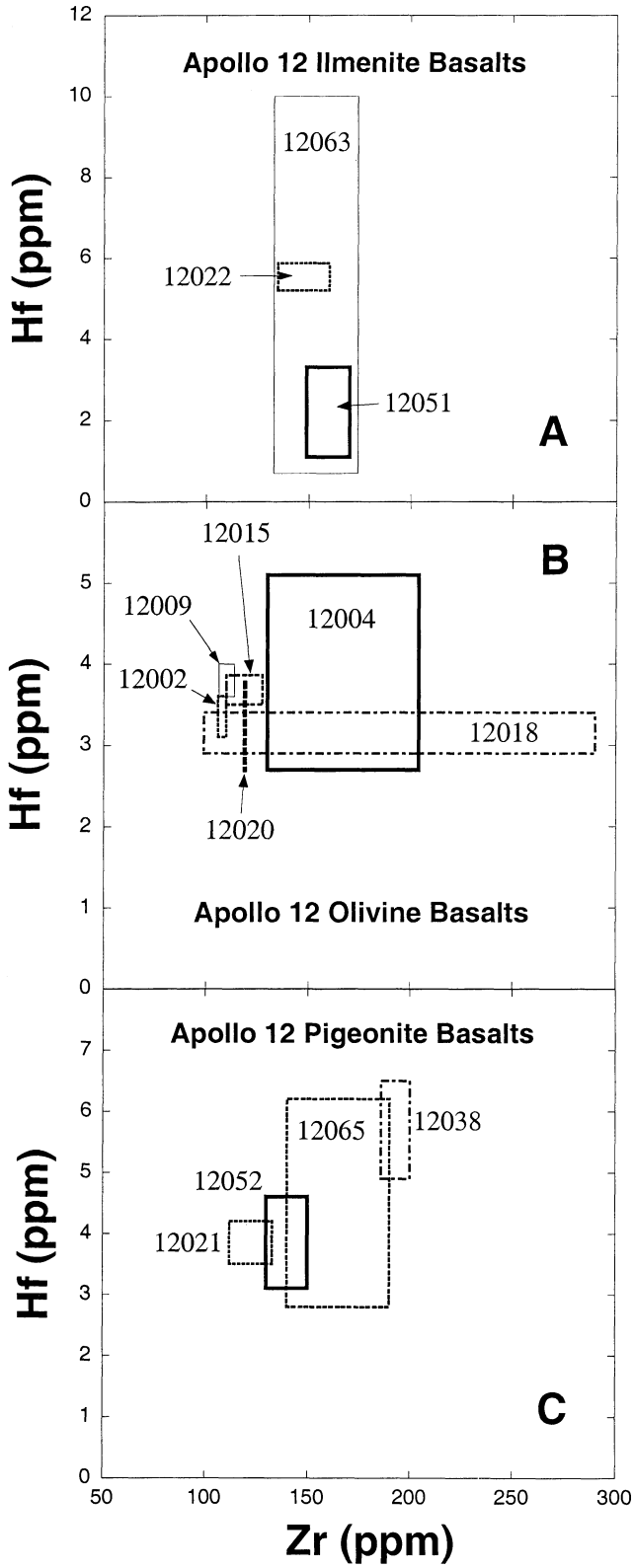

Figure 1. Literature data for Apollo 12 low-Ti mare basalts demonstrating the range in Zr and Hf concentrations and thus Zr/Hf ratios for individual basalts. Data sources are given by *Neal and Taylor* [1992].

earlier than assumed from the LMO or HFSE partitioning into Ti oxides on the Moon was different from what is observed in natural and synthetic systems on Earth.

In this study the mare basalt database has been carefully examined, and only those data obtained from the same aliquot of material have been used in petrogenetic interpretations. This should reduce the ambiguity of interpreting elemental ratios. New trace element data from the Notre Dame ICP-MS facility (see http://www.nd.edu/~icpmslab) are presented for the mare basalts.

3. Mare Basalts: New Data

New data obtained by ICP-MS are presented in Table 1. While the new data have reduced scatter in some HFSE correlations, it is recognized that analyses of only 65 basalts are reported here. However, the advantage of ICP-MS is that it can analyze practically all of the trace elements of petrogenetic interest from the same aliquot. This removes the random error of sample heterogeneity when element ratios, such as Zr/Hf and Nb/Ta, are calculated using data from different aliquots analyzed by different methods (see above).

3.1. Analytical Method

Between 0.7 and 1 g of sample was crushed in an attempt to reduce the effects of sample heterogeneity. Crushing was conducted using an agate pestle and mortar that had been cleaned prior to using in the lunar study by soaking in ultrapure 8 N HNO_3 for 1 week on a hot plate at 150°C and then rinsing in 18 megaohm ultrapure water. The pestle and mortar were thoroughly washed in ultrapure water between samples and dried to avoid sample cross contamination. All crushing was conducted in a Class 1000 clean laboratory.

All acids used in the dissolution procedure were purchased at reagent grade and then double-distilled in-house to ensure purity. Approximately 50 mg of each sample were dissolved in a mixture of 60 drops of 29 N HF and 40 drops of 16 N HNO_3. Samples were sealed in Teflon dissolution vessels and placed on a hot plate at 150°C over night, then removed and allowed to cool. The caps were then removed, and any solution adhering to the cap was washed back into the vessel with ultrapure water. The solution was then placed back on the hot plate and evaporated till dry. Approximately 2 mL of 16 N HNO_3 were added and each sample was capped and placed back on the hot plate and left overnight after agitation to ensure that the dried sample mixed with the acid. The samples were then removed from the hot plate and allowed to cool. The caps were removed, and adhering sample solution was washed back into the vessel with ultrapure water. The solution was then placed back on the hot plate and dried. A further 2 mL of 16 N HNO_3 were added and the solution was agitated before being immediately dried down. A final 2 mL of 16 N HNO_3 were added plus 2 mL of 18 megaohm water, and the sample was completely dissolved. This solution was brought up to 100 g by transferring to 125 mL polypropylene bottles and adding 0.8 N HNO_3 to give ~0.05% of rock in solution.

The analytical protocol is one modified from *Jenner et al.* [1990]. Internal standards of As, Rh, In, Re, and Tl were used at 20 ppb in all solutions. Stock solutions of Standards A and B were prepared at double the concentrations shown in Table 2. Each standard was prepared by adding 3 g of a stock solution to a test tube followed by 3 g of the internal standard stock. The standard concentration for each element in the final solution should be close to those given in Table 2. A stock solution of the spike was prepared (Table 2). In this stock solution were the internal standards at 40 ppb concentration. Three grams of this solution are added to 3 g of sample or concentration standard, such that the concentrations are half those in Table 2 and the internal standards are again at 20 ppb.

Table 1. Trace element data gathered via ICP-MS[a].

Sample, Subsample	10003, 178	10017, 352	10044, 638	10049, 90	10050, 165	10057, 268	10058, 250	10069, 89	10092, 14	12004, 134	12007, 14	12008, 59	12009, 130	12011, 29	12015, 25
Li	na	na	2.56	8.02	0.41	na	na	na	na	na	na	na	7.21	8.39	na
Be	1.00	2.24	2.10	3.10	1.84	1.82	1.78	2.62	1.09	0.73	1.27	1.11	0.62	0.80	0.43
Sc	75.5	75.4	90.9	75.4	114.2	77.2	88.6	71.6	85.6	43.0	55.9	56.2	45.7	51.7	44.1
V	48.9	47.6	45.2	40.5	115	45.5	65.3	50.2	96.0	136	152	164	186	180	118
Cr	1268	2019	1168	1692	2445	2063	1201	2122	2446	3588	2438	3908	4249	3632	2820
Co	15.7	27.9	14.3	25.2	18.1	26.8	15.5	27.7	21.4	52.7	31.6	63.2	na	na	52.6
Ni	8.32	6.37	1.46	6.34	2.17	5.91	1.15	7.71	3.60	63.5	4.39	64.3	61.0	37.3	56.5
Cu	37.6	32.8	37.6	49.9	55.9	60.5	37.6	35.1	43.7	11.6	18.3	20.8	12.8	12.1	12.4
Zn	58.4	73.6	64.1	77.4	99.0	75.6	88.1	66.5	72.7	14.7	26.0	28.5	6.64	6.81	17.1
Ga	4.02	4.90	4.97	4.90	5.02	4.19	4.52	2.94	3.64	2.77	3.65	3.44	2.82	3.08	2.83
Rb	0.79	5.22	1.22	7.27	1.11	5.27	0.88	5.84	0.81	1.31	1.75	0.90	1.08	1.18	0.94
Sr	148.8	142.7	215.0	177.3	216.4	144.1	217.3	155.6	143.8	83.0	135.4	144.5	99.6	114.6	90.1
Y	117.0	147.3	158.6	197.4	165.4	175.8	111.4	271.4	92.1	32.9	54.1	54.7	34.2	39.0	37.2
Zr	338.8	629.9	333.6	472.5	380.7	523.3	299.8	715.5	210.0	98.3	146.1	117.7	112.3	119.9	101.7
Nb	20.3	25.1	28.4	30.3	29.6	26.7	24.7	39.3	18.2	6.93	10.1	6.70	6.54	7.51	6.78
Mo	0.18	0.99	0.12	0.12	0.16	0.07	0.19	0.26	0.06	0.08	0.51	0.22	0.15	0.10	0.12
Sb	0.04	0.02	0.03	0.23	0.06	0.02	bdl	0.04	0.02	0.01	bdl	bdl	bdl	bdl	0.02
Cs	0.05	0.37	0.02	0.16	0.01	0.36	0.05	0.39	0.03	0.13	0.05	0.01	0.04	0.06	0.10
Ba	103.1	243.4	118.5	309.5	118.5	261.0	108.5	282.2	73.2	56.5	90.5	59.1	63.4	72.9	64.3
La	17.5	23.2	11.7	28.0	11.9	23.4	11.5	27.0	8.03	6.00	8.26	5.80	5.86	6.84	5.49
Ce	55.6	81.8	42.1	82.1	38.4	83.3	45.4	85.2	24.9	16.7	22.7	15.7	16.3	18.5	16.9
Pr	7.96	11.2	7.75	12.9	7.19	11.1	7.33	11.6	4.41	2.30	3.49	2.62	2.58	2.90	2.34
Nd	44.4	61.6	43.1	63.8	40.5	59.4	42.9	67.0	23.2	11.8	17.0	13.6	12.4	14.0	12.6
Sm	15.6	21.2	17.1	21.9	16.1	20.1	18.2	23.0	9.15	4.37	5.68	5.11	4.26	4.90	4.51
Eu	1.87	2.03	2.76	2.27	2.37	1.95	2.40	2.16	1.57	0.83	1.21	1.17	0.89	1.01	0.75
Gd	20.5	27.7	24.6	29.8	22.8	26.4	23.3	29.0	13.4	5.69	7.82	7.23	6.33	7.43	5.77
Tb	3.60	4.80	4.23	5.22	4.04	4.53	4.50	5.19	2.37	1.03	1.35	1.28	1.00	1.17	1.01
Dy	22.8	29.8	27.7	35.1	26.6	29.3	28.1	34.6	16.0	6.55	8.87	8.68	6.96	7.77	6.52
Ho	4.79	6.31	5.64	7.23	5.33	6.50	5.56	7.04	3.34	1.35	1.86	1.79	1.40	1.60	1.34
Er	14.0	17.7	16.0	21.3	15.2	17.8	16.1	19.4	9.73	3.79	5.44	5.27	4.11	4.65	3.89
Tm	1.85	2.39	2.20	2.93	2.07	2.43	2.25	2.77	1.39	0.53	0.72	0.71	0.57	0.66	0.54
Yb	13.2	17.3	14.4	19.0	13.5	17.0	15.3	20.2	9.03	3.66	4.75	4.68	3.68	4.37	3.53
Lu	1.84	2.12	1.90	2.57	1.75	2.26	2.07	2.47	1.23	0.48	0.63	0.61	0.50	0.57	0.51
Hf	10.2	14.0	11.7	16.9	11.2	13.6	11.2	15.7	7.56	2.97	4.24	3.62	3.26	3.69	2.87
Ta	1.32	1.69	1.67	1.86	1.55	1.76	1.82	1.87	1.18	0.51	0.54	0.34	0.40	0.46	0.40
W	0.22	.51	0.16	0.32	0.13	0.52	0.16	0.53	0.07	0.14	0.14	0.04	0.17	0.20	0.16
Pb	0.51	1.27	0.52	2.95	0.76	1.43	0.55	1.52	0.40	0.31	0.55	0.21	0.31	0.39	0.38
Th	0.94	2.66	0.86	3.78	0.74	2.77	0.74	3.28	0.68	0.69	1.19	0.59	0.90	0.98	0.72
U	0.28	0.77	0.24	0.91	0.22	0.76	0.23	0.88	0.22	0.22	0.31	0.15	0.24	0.24	0.22

Table 1. (continued)

Sample, Subsample	12020, 515	12021, 581	12022, 278	12031, 37	13038, 244	12045, 20	12051, 226	12053, 274	12054, 6	12063, 325	12064, 20	14053, 237	14072, 44	15016, 206	15119, 23
Li	na	na	9.27	3.85	na	na	na	na	na	na	6.21	na	na	6.73	7.89
Be	1.03	0.62	0.87	0.81	1.22	1.22	1.51	0.81	1.29	1.34	1.04	0.42	1.12	0.60	0.80
Sc	47.0	54.1	59.6	49.5	50.4	58.9	63.7	54.0	78.5	64.7	61.7	54.1	57.3	41.8	58.0
V	182	117	156	128	133	162	161	167	193	167	140	111	117	304	447
Cr	3615	2295	3004	1934	2221	3757	2547	3312	2841	3575	2097	2168	3558	5867	6251
Co	66.1	34.4	na	28.0	32.4	53.2	40.5	41.7	38.9	54.1	35.4	32.0	40.8	57.9	65.2
Ni	89.3	6.71	29.1	4.21	4.42	51.3	13.9	18.6	9.09	41.5	4.10	13.6	47.2	74.7	64.4
Cu	16.5	15.4	15.7	14.0	18.9	20.3	23.8	16.3	26.6	23.5	23.1	16.3	17.2	13.8	19.8
Zn	22.6	26.1	11.3	16.9	23.8	28.9	34.5	23.2	37.3	31.6	31.0	23.7	20.1	18.3	21.7
Ga	3.35	3.69	3.64	3.43	4.84	3.37	4.32	3.60	4.15	3.78	4.06	2.54	3.13	3.65	4.52
Rb	1.13	0.96	0.78	1.09	0.67	0.88	1.24	1.31	1.14	0.93	1.19	1.95	1.53	0.94	1.24
Sr	105.1	112.2	147.5	126.9	207.3	151.0	163.0	115.6	171.3	158.1	144.6	95.2	83.3	97.2	123.2
Y	42.8	39.3	50.7	35.9	59.8	57.3	59.2	43.2	64.7	60.6	50.0	49.7	46.8	31.0	36.8
Zr	119.2	109.3	121.7	92.5	184.7	125.4	132.7	149.3	221.5	129.9	141.7	183.8	141.1	108.9	153.8
Nb	8.45	8.75	5.98	6.50	9.29	6.80	8.57	9.81	8.71	7.35	8.71	15.4	13.6	7.52	7.50
Mo	1.12	0.12	0.11	bdl	0.03	bdl	0.11	0.52	bdl	bdl	bdl	bdl	0.44	0.08	0.03
Sb	0.03	0.04	bdl	bdl	bdl	bdl	0.12	0.05	bdl	bdl	0.21	0.03	bdl	bdl	0.01
Cs	0.02	0.06	0.03	0.05	bdl	0.02	0.10	0.06	0.03	0.03	0.01	0.10	0.05	0.02	0.02
Ba	64.2	67.1	56.8	58.5	122.0	57.5	74.7	71.1	73.2	64.2	73.9	151.1	105.3	55.8	60.6
La	5.87	6.48	5.59	5.22	12.0	5.60	7.22	6.41	7.13	6.13	6.77	12.4	7.96	5.87	5.86
Ce	17.6	20.2	16.9	15.6	30.8	17.0	20.1	18.9	19.7	17.6	18.4	36.5	20.8	14.9	16.9
Pr	2.53	2.82	2.93	2.40	4.64	2.93	3.18	2.66	3.30	2.98	2.84	4.63	3.10	2.24	2.54
Nd	12.9	15.6	15.3	11.4	22.0	14.8	15.4	14.2	16.7	15.1	14.1	22.5	14.1	10.5	11.9
Sm	4.38	5.81	5.63	3.93	6.91	5.54	5.70	4.92	6.11	5.84	5.06	6.60	4.45	3.42	4.03
Eu	0.73	1.13	1.30	1.04	1.99	1.27	1.38	0.97	1.37	1.29	1.156	1.06	0.97	0.87	0.98
Gd	5.78	7.70	8.74	5.40	9.28	7.97	8.06	7.00	8.65	8.15	7.17	8.33	6.12	4.53	5.59
Tb	1.11	1.36	1.48	0.94	1.48	1.45	1.49	1.21	1.54	1.45	1.23	1.52	1.08	0.80	0.88
Dy	7.11	8.52	10.2	6.35	9.77	9.79	9.52	7.45	10.2	9.88	8.40	9.36	7.35	5.10	5.72
Ho	1.41	1.63	2.09	1.33	1.94	1.98	2.05	1.61	2.12	2.03	1.71	2.05	1.59	1.00	1.07
Er	3.82	4.87	6.13	3.88	5.52	5.74	5.68	4.44	6.15	5.96	4.92	5.96	4.71	2.77	3.00
Tm	0.53	0.66	0.84	0.53	0.74	0.80	0.89	0.59	0.87	0.86	0.69	0.82	0.72	0.38	0.40
Yb	3.60	4.47	5.51	3.48	4.67	5.44	5.16	4.23	5.54	5.41	4.61	6.19	4.69	2.38	2.50
Lu	0.52	0.59	0.77	0.48	0.61	0.68	0.73	0.55	0.73	0.71	0.57	0.80	0.63	0.31	0.34
Hf	3.12	3.62	4.25	2.87	4.70	4.17	4.22	3.55	5.70	4.29	4.10	4.92	3.87	2.58	3.35
Ta	0.44	0.53	0.39	0.39	0.55	0.38	0.58	0.49	0.44	0.41	0.45	0.85	0.75	0.46	0.56
W	0.11	0.13	0.16	0.11	0.10	0.09	0.14	0.12	0.08	0.07	0.06	0.22	0.14	bdl	0.08
Pb	0.29	0.39	0.29	0.44	0.14	0.17	0.36	0.45	0.25	0.31	0.56	2.33	0.87	0.11	bdl
Th	0.77	0.87	0.63	0.82	0.61	0.64	0.97	0.81	0.78	0.71	0.83	1.51	1.13	0.26	bdl
U	0.22	0.29	0.19	0.22	0.16	0.17	0.34	0.26	0.23	0.20	0.23	0.48	0.31	0.08	bdl

Table 1. (continued)

Sample, Subsample	15256, 78	15379, 29	15529, 18	15535, 159	15536, 20	15545, 100	15546, 23	15547, 20	15555, 924	15555, 925	15556, 198	15556, 199	15557, 145	15598, 21	15607, 24
Li	7.22	7.04	7.15	7.02	6.70	8.30	7.02	7.00	6.57	6.12	7.29	7.05	6.60	6.59	7.21
Be	0.62	0.42	0.56	0.44	0.66	0.54	0.64	0.62	0.44	0.50	0.62	0.55	0.62	0.43	0.48
Sc	46.9	41.3	44.3	48.4	50.6	43.9	43.3	51.8	44.2	43.8	52.0	46.6	52.2	47.5	46.9
V	258	213	249	263	359	308	254	316	224	317	258	266	316	204	213
Cr	4082	4319	4168	5094	6419	6444	4323	6253	4760	5099	6177	5555	4759	3923	4269
Co	58.6	54.1	53.0	68.6	73.5	61.5	58.2	71.3	65.3	66.4	59.2	54.6	62.8	56.6	61.8
Ni	68.3	68.0	52.8	83.0	93.4	70.4	65.8	85.6	78.4	81.3	81.7	61.1	64.0	57.4	67.4
Cu	16.9	14.1	16.1	14.5	23.5	14.3	16.8	15.4	14.4	13.6	17.3	15.5	19.0	19.6	15.8
Zn	21.3	17.0	22.3	18.0	22.7	19.7	20.6	19.4	15.5	16.6	21.0	16.8	21.5	24.5	20.3
Ga	4.17	3.85	3.89	3.79	4.15	3.57	3.89	3.89	3.74	3.90	4.22	3.95	4.46	4.21	4.05
Rb	1.06	0.97	0.92	0.87	1.07	0.87	1.02	1.04	0.99	0.80	0.99	1.00	1.06	0.98	0.99
Sr	114.8	100.1	103.3	108.7	109.4	106.3	106.3	106.6	104.5	109.7	114.1	114.4	123.1	116.9	111.5
Y	33.3	28.5	29.4	28.9	33.5	29.3	31.7	31.5	30.4	27.4	33.7	32.4	34.6	30.4	31.0
Zr	115.1	95.6	100.5	90.5	113.3	89.2	107.3	115.2	99.9	90.6	112.3	108.5	115.7	108.0	99.3
Nb	7.89	6.47	6.65	6.48	7.83	6.31	6.94	7.12	6.94	5.77	7.02	7.30	7.42	7.23	6.88
Mo	0.32	0.06	0.12	0.20	0.61	0.04	0.10	0.36	0.26	0.12	0.08	0.18	0.10	0.03	0.17
Sb	bdl	0.01	bdl	0.01	bdl	bdl	bdl	0.04	0.03	0.02	bdl	0.01	bdl	bdl	0.03
Cs	0.03	0.04	0.15	0.02	0.03	0.02	0.03	0.03	0.03	0.01	0.05	0.04	0.01	0.04	0.03
Ba	67.2	55.2	55.4	53.8	56.7	49.2	60.2	55.4	56.7	49.9	59.9	57.1	60.4	56.4	58.9
La	6.41	5.40	5.39	5.20	5.58	4.60	5.89	5.28	5.54	4.73	5.79	5.46	5.93	5.64	5.62
Ce	15.8	14.2	14.8	13.2	14.5	13.4	15.7	15.1	14.5	11.8	15.4	15.4	14.9	14.0	14.4
Pr	2.38	2.14	2.18	2.08	2.18	2.02	2.29	2.28	2.23	1.79	2.33	2.35	2.24	2.22	2.24
Nd	11.2	10.5	9.98	9.21	9.94	9.30	10.7	10.5	10.5	8.40	10.7	11.1	10.4	10.2	10.3
Sm	3.80	3.40	3.42	3.06	3.43	3.41	3.57	3.59	3.55	2.73	3.60	3.73	3.72	3.46	3.44
Eu	0.94	0.89	0.87	0.81	0.86	0.83	0.95	0.87	0.89	0.78	0.92	0.95	0.93	0.89	0.91
Gd	4.87	4.55	4.60	4.18	4.49	4.44	4.99	4.80	4.57	3.61	4.81	4.92	4.78	4.50	4.79
Tb	0.86	0.77	0.79	0.72	0.77	0.73	0.83	0.82	0.78	0.64	0.85	0.82	0.85	0.78	0.77
Dy	5.39	4.96	5.05	4.61	4.69	4.57	5.41	5.04	5.04	4.08	5.44	5.34	5.18	4.92	5.17
Ho	1.05	0.98	0.99	0.90	0.95	0.91	1.03	0.97	0.98	0.81	1.09	1.04	1.00	0.98	1.00
Er	2.97	2.69	2.83	2.47	2.56	2.46	3.05	2.72	2.71	2.25	2.98	2.83	2.78	2.65	2.77
Tm	0.40	0.35	0.36	0.32	0.36	0.31	0.38	0.36	0.38	0.31	0.39	0.39	0.38	0.36	0.37
Yb	2.52	2.31	2.38	2.11	2.15	2.12	2.54	2.30	2.40	1.94	2.51	2.39	2.49	2.30	2.42
Lu	0.30	0.29	0.30	0.28	0.28	0.27	0.33	0.29	0.31	0.25	0.31	0.33	0.29	0.31	0.30
Hf	2.69	2.54	2.63	2.30	2.42	2.15	2.83	2.63	2.53	2.24	2.68	3.02	2.65	2.79	2.56
Ta	0.47	0.38	0.51	0.41	0.47	0.36	0.44	0.40	0.50	0.40	0.45	0.59	0.48	0.41	0.51
W	0.03	bdl	0.05	bdl	0.03	0.01	0.01	bdl	0.05	bdl	0.01	0.11	0.08	bdl	0.04
Pb	0.21	0.62	0.07	0.23	0.60	0.22	0.37	0.24	0.22	0.32	0.19	0.19	bdl	0.57	0.24
Th	0.36	0.53	0.07	0.48	0.76	0.41	0.59	0.49	0.54	0.72	0.43	0.52	0.34	0.52	0.51
U	0.10	0.14	0.02	0.12	0.22	0.12	0.18	0.12	0.15	0.25	0.13	0.14	0.10	0.13	0.14

Table 1. (continued)

Sample	15622,	15630,	15636,	15647,	15668,	15672,	15674,	15675,	15676,	15683,	70135,	70275,	70315,	74235,	74245,
Subsample	22	9	26	20	22	25	17	11	21	17	93	47	30	62	34
Li	6.00	7.16	7.14	7.00	7.17	6.33	7.22	7.42	6.74	7.12	na	na	na	na	na
Be	0.52	0.43	0.42	0.49	0.49	0.50	0.58	0.42	0.51	0.48	0.77	0.84	0.60	0.53	0.84
Sc	49.6	38.4	41.4	49.6	44.7	40.3	48.2	43.6	47.1	46.7	70.0	79.7	79.2	85.5	73.8
V	330	208	222	275	197	255	254	247	254	220	103	75.8	146	137	139
Cr	8046	5563	5325	5228	3397	4840	4229	5875	4195	4018	3124	1727	2790	2906	3399
Co	72.7	59.3	70.2	65.9	55.9	57.2	55.9	52.7	58.1	59.4	27.9	16.7	24.3	22.7	27.7
Ni	98.7	81.2	99.6	71.5	57.2	73.7	56.5	52.6	59.9	64.8	3.35	1.03	2.22	2.16	8.90
Cu	14.6	13.3	13.7	15.7	13.8	12.0	16.9	16.4	18.2	15.7	36.5	36.1	49.5	49.6	51.6
Zn	17.6	15.1	17.0	19.6	23.5	17.5	20.4	21.7	22.3	24.1	74.7	83.6	119.3	106.4	110.6
Ga	3.99	3.34	3.78	4.07	4.19	3.21	3.88	3.64	3.92	4.11	3.32	4.08	3.75	3.92	3.46
Rb	1.01	0.91	0.78	1.05	0.92	0.82	1.00	1.07	1.02	0.99	0.52	0.59	0.24	0.60	1.08
Sr	110.9	96.5	104.6	117.0	99.0	96.4	112.2	122.6	115.5	111.2	166.9	154.9	162.7	198.8	159.1
Y	33.9	28.1	26.1	32.2	27.9	27.1	31.9	35.8	32.8	31.8	98.6	82.7	66.3	133.6	83.6
Zr	111.4	96.5	116.5	108.5	87.0	92.8	111.7	125.0	118.1	105.3	255.7	184.0	196.9	255.6	218.5
Nb	7.63	6.36	6.29	7.35	7.43	5.82	7.35	7.84	7.22	7.27	19.3	19.1	20.7	26.6	20.7
Mo	0.12	0.09	0.07	0.08	0.09	0.04	0.21	0.54	0.03	0.07	0.03	0.22	bdl	0.15	0.40
Sb	0.01	0.01	0.02	0.01	0.26	bdl	bdl	0.06	bdl	0.01	0.03	0.02	bdl	0.02	bdl
Cs	0.03	0.02	0.02	0.03	0.03	0.02	0.03	0.03	0.12	0.03	bdl	bdl	bdl	bdl	0.04
Ba	61.1	55.2	52.3	59.1	53.2	49.1	57.9	58.6	59.8	59.6	56.1	67.3	53.8	83.0	65.2
La	6.29	5.69	4.92	5.89	5.19	4.98	5.69	5.65	5.72	5.80	4.28	5.95	3.78	6.50	5.83
Ce	14.6	15.2	12.1	14.6	14.5	13.5	14.9	15.6	14.9	15.0	17.1	21.3	16.2	25.5	23.3
Pr	2.24	2.29	1.87	2.21	2.23	2.07	2.29	2.39	2.28	2.31	2.87	3.54	2.74	4.35	3.77
Nd	10.4	10.5	8.48	10.4	10.4	9.21	10.7	11.4	10.5	11.0	18.6	20.3	17.7	25.9	22.7
Sm	3.50	3.56	2.94	3.66	3.57	3.23	3.56	3.70	3.66	3.60	7.94	8.34	7.48	10.7	9.44
Eu	0.85	0.86	0.79	0.87	0.93	0.79	0.94	0.95	0.89	0.92	1.72	1.57	1.60	1.95	1.73
Gd	4.63	4.62	3.69	4.75	4.93	4.10	4.70	5.18	4.78	4.73	11.8	12.1	9.73	13.9	13.3
Tb	0.80	0.79	0.65	0.77	0.83	0.70	0.82	0.85	0.81	0.81	2.17	2.09	1.99	2.82	2.56
Dy	4.91	5.00	4.12	5.01	5.20	4.63	5.16	5.52	5.18	5.27	13.7	13.4	13.8	18.4	16.0
Ho	0.96	0.99	0.80	0.95	1.01	0.90	1.01	1.05	1.02	1.00	2.76	2.98	2.68	3.95	3.30
Er	2.71	2.72	2.19	2.77	2.90	2.52	2.87	2.92	2.85	2.72	7.85	8.06	7.76	11.1	9.32
Tm	0.36	0.36	0.30	0.37	0.39	0.34	0.37	0.38	0.37	0.38	1.06	1.13	1.05	1.53	1.28
Yb	2.29	2.28	1.86	2.33	2.47	2.16	2.46	2.50	2.42	2.38	7.67	8.07	7.88	11.1	8.47
Lu	0.29	0.29	0.25	0.31	0.32	0.26	0.31	0.31	0.32	0.31	1.05	1.13	1.06	1.42	1.12
Hf	2.53	2.54	2.79	2.67	2.77	2.39	2.79	2.72	2.77	2.75	6.77	6.34	6.39	8.78	7.65
Ta	0.46	0.41	0.41	0.50	0.43	0.44	0.51	0.49	0.51	0.46	1.40	1.32	1.44	1.79	1.47
W	bdl	0.03	bdl	0.08	0.04	bdl	bdl	0.06	bdl	0.05	0.09	0.10	bdl	0.08	0.04
Pb	0.20	0.23	0.20	0.19	0.19	0.01	0.14	0.60	0.42	0.25	0.23	0.29	0.15	0.40	0.25
Th	0.52	0.59	0.43	0.50	0.51	0.01	0.16	0.50	0.38	0.51	0.23	0.36	0.23	0.36	0.38
U	0.14	0.16	0.12	0.13	0.11	bdl	0.05	0.13	0.12	0.14	0.09	0.12	0.07	0.10	0.12

Table 1. (continued)

Sample Subsample	74255, 181	74275, 48	78575, 7	78585, 15	78598, 6	BHVO-1 (Cert)	Average (n=10)	Standard Deviation
Li	na	na	na	na	na	4.6	4.59	0.13
Be	1.02	0.98	0.85	0.33	1.11	1.1	0.95	0.11
Sc	75.0	66.3	87.1	108.1	81.3	31.8	31.4	2.1
V	103	103	79.3	109	111	317	313	43.4
Cr	4147	3303	3260	2605	3361	289	291	27.8
Co	24.7	21.2	20.9	24.5	19.8	45	48.2	2.1
Ni	5.55	4.78	3.68	3.39	1.86	121	120.1	6.3
Cu	36.0	48.7	37.3	44.1	43.3	136	146.7	12.2
Zn	84.3	74.2	89.4	95.2	88.0	105	113.6	12.3
Ga	3.60	2.97	3.86	3.97	3.77	21	21.4	1.0
Rb	1.21	1.40	0.27	0.43	0.65	11[b]	9.54	0.75
Sr	169.2	141.4	157.4	152.4	183.0	403	401	14
Y	110.7	83.3	91.0	132.5	101.8	27.6[b]	24.2	0.6
Zr	275.8	200.6	256.6	272.0	230.3	179	174	7.3
Nb	25.3	19.5	23.3	32.0	23.3	19	19.4	0.6
Mo	0.03	0.02	0.03	0.16	bdl	1.02	1.04	0.07
Sb	bdl	bdl	0.01	bdl	0.03	0.16	0.16	0.03
Cs	0.03	0.02	bdl	bdl	0.03	0.13	0.11	0.02
Ba	72.1	66.4	69.5	62.1	80.7	139	134	3.3
La	6.47	5.78	5.28	5.66	6.31	15.8	15.8	0.6
Ce	24.8	22.8	21.1	19.5	23.7	39	40.1	0.8
Pr	4.08	4.32	3.38	3.20	4.06	5.7	5.56	0.22
Nd	26.4	24.3	22.5	18.5	23.2	25.2	24.9	0.5
Sm	12.1	10.1	9.16	7.43	9.85	6.2	6.32	0.17
Eu	1.90	1.81	1.77	1.39	1.96	2.1	2.07	0.07
Gd	16.9	14.5	13.6	9.76	15.5	6.4	6.62	0.10
Tb	2.80	2.57	2.56	1.95	2.67	0.96	0.94	0.02
Dy	17.8	17.0	17.1	12.7	17.5	5.2	5.39	0.22
Ho	3.53	3.49	3.54	2.79	3.42	0.99	0.99	0.03
Er	9.54	10.3	9.78	7.52	9.84	2.4	2.55	0.13
Tm	1.40	1.39	1.41	1.02	1.35	0.33	0.33	0.02
Yb	10.0	9.17	9.74	7.74	9.42	2.02	2.06	0.08
Lu	1.31	1.20	1.27	1.00	1.39	0.291	0.26	0.02
Hf	8.58	8.96	7.23	6.17	8.04	4.38	4.50	0.20
Ta	1.55	1.51	1.43	1.47	1.56	1.23	1.34	0.26
W	0.15	0.03	0.09	0.06	0.09	0.2	0.23	0.08
Pb	0.33	0.68	0.28	0.20	0.21	2.6[b]	2.29	0.46
Th	0.42	0.47	0.30	0.37	0.32	1.08[b]	1.21	0.23
U	0.16	0.12	0.10	0.21	0.11	0.42	0.44	0.08

[a] All concentrations are in ppm. Here, bdl is below detection limit; na is not analyzed.
[b] Reference values for BHVO-1 are being revised. See http://www.nd.edu/~icpmslab for details.
Lithium is not reported for some basalts owing to the high background from prior analyses of samples fused with lithium metaborate.

Two sets of tubes for each standard reference material and each unknown sample were prepared along with two test tubes of each concentration standard (1, 5, 10, 50, 100 ppb). Each tube contained 3 g of concentration standard solution at double the concentration required (i.e., 2, 10, 20, 100, or 200 ppb). To one tube were added 3 g of the internal standard stock solution and to the other were added 3 g of the spike stock solution containing the internal standards at 40 ppb. This gave concentration standards of 1, 5, 10, 50, and 100 ppb, the former unspiked (except for the internal standards now at 20 ppb) and the latter spiked with all elements listed in Table 2 (plus the internal standards at 20 ppb). Throughout this and the next two steps, the former is the unspiked aliquot and the latter is the spiked aliquot. Procedural blanks, acid blanks, and sample solutions were treated in the same way.

The analysis order of the tubes is critical in order to monitor drift and interferences. The order is given in Table 3. Between each tube, a three-stage wash sequence was run: (1) 1.6 N HNO_3 + 1 drop of 29 N HF per 150 mL of HNO_3; (2) 1.6 N HNO_3; and (3) 0.8 N HNO_3. Each wash was run for 90 s (see *McGinnis et al.* [1997] for full details). Reference material BHVO-1 was run at the beginning, middle, and end of each run. Each run is terminated with Standard A, Standard B, then the concentration standards of 1, 5, 10, 50, and 100 ppb (unspiked and spiked).

Using this procedure, memory effects and machine drift are monitored. The procedure allows for blank and interference cor-

Table 2. Standard and Spike Concentrations Used in Trace Element ICP-MS Analysis[a].

Element	Standard A	Standard B	Spike
Li	40	--	--
Be	40	--	40
Sc	40	--	80
V	40	--	80
Cr	--	100	--
Co	40	--	80
Ni	40	--	80
Cu	40	--	80
Zn	40	--	80
Ga	--	40	80
Rb	40	40	--
Sr	100	--	200
Y	20	--	20
Zr	40	--	80
Nb	20	--	20
Mo	20	--	20
Sb	20	--	20
Cs	20	20	20
Ba	200	--	400
La	20	--	40
Ce	20	20	--
Pr	20	--	40
Nd	--	40	80
Sm	--	40	80
Eu	--	40	20
Gd	--	40	40
Tb	40	--	20
Dy	20	--	40
Ho	20	--	20
Er	40	--	80\
Tm	20	--	40
Yb	20	--	20
Lu	--	40	20
Hf	--	20	40
Ta	--	20	20
W	--	20	20
Pb	40	--	40
Th	20	20	20
U	20	--	20

[a] Concentrations are in ng/g (ppb).

rections to be made, as well as fluctuations in sensitivity. The final data are calculated using a combination of external calibration and standard addition [see *Jenner et al.*, 1990].

3.2. Results

The new data can be used to examine source composition by looking at elemental ratios that are not modified by fractional crystallization. Ratios involving the HFSEs are the most useful (Figure 2). Use of these ratios has been heretofore limited owing to the analytical problems (see above). The new data are generally consistent with those of *Hughes and Schmitt* [1985] but suggest that a refinement of petrogenetic models proposed by *Chyi and Ehmann* [1973], *Ehmann et al.* [1975], and *Garg and Ehmann* [1976] is required. The new data indicate that the low-Ti mare basalts contain approximately chondritic Zr/Hf ratios (Figure 2a), while the high-Ti basalts exhibit, on average, slightly lower values, with KREEP exhibiting consistently suprachondritic values. A similar scenario is seen with Zr/Nb and Nb/Ta (Figures 2b and 2c), although KREEP exhibits approximately chondritic values for Zr/Nb. The new data demonstrate that the

Table 3. Protocol for ICP-MS trace element analyses[a].

Sequence	Analyte
1)	Standard A
2)	Standard B
3)	5% HNO_3 Acid Blank
4)	1ppb Conc Std Unsp
5)	1ppb Conc Std Sp
6)	25% HNO_3 Acid Blank
7)	5ppb Conc Std Unsp
8)	5ppb Conc Std Sp
9)	5% HNO_3 Acid Blank
10)	10ppb Conc Std Unsp
11)	10ppb Conc Std Sp
12)	5% HNO_3 Acid Blank
13)	Standard A
14)	Standard B
15)	50ppb Conc Std Unsp
16)	50ppb Conc Std Sp
17)	5% HNO_3 Acid Blank
18)	100ppb Conc Std Unsp
19)	100ppb Conc Std Sp
20)	5% HNO_3 Acid Blank
21)	Procedural Blank Unsp
22)	Procedural Blank Sp
23)	5% HNO_3 Acid Blank
24)	Standard A
25)	Standard B
26)	5% HNO_3 Acid Blank
27)	Std Ref. Material Unsp
28)	Std Ref. Material Sp
29)	5% HNO_3 Acid Blank
30)	Unknown Sample 1 Unsp
31)	Unknown Sample 1 Sp
32)	5% HNO_3 Acid Blank
33)	Unknown Sample 2 Unsp
34)	Unknown Sample 2 Sp
35)	5% HNO_3 Acid Blank
36)	Standard A
37)	Standard B
38)	5% HNO_3 Acid Blank

[a] Unsp = Unspiked; Sp = Spiked.

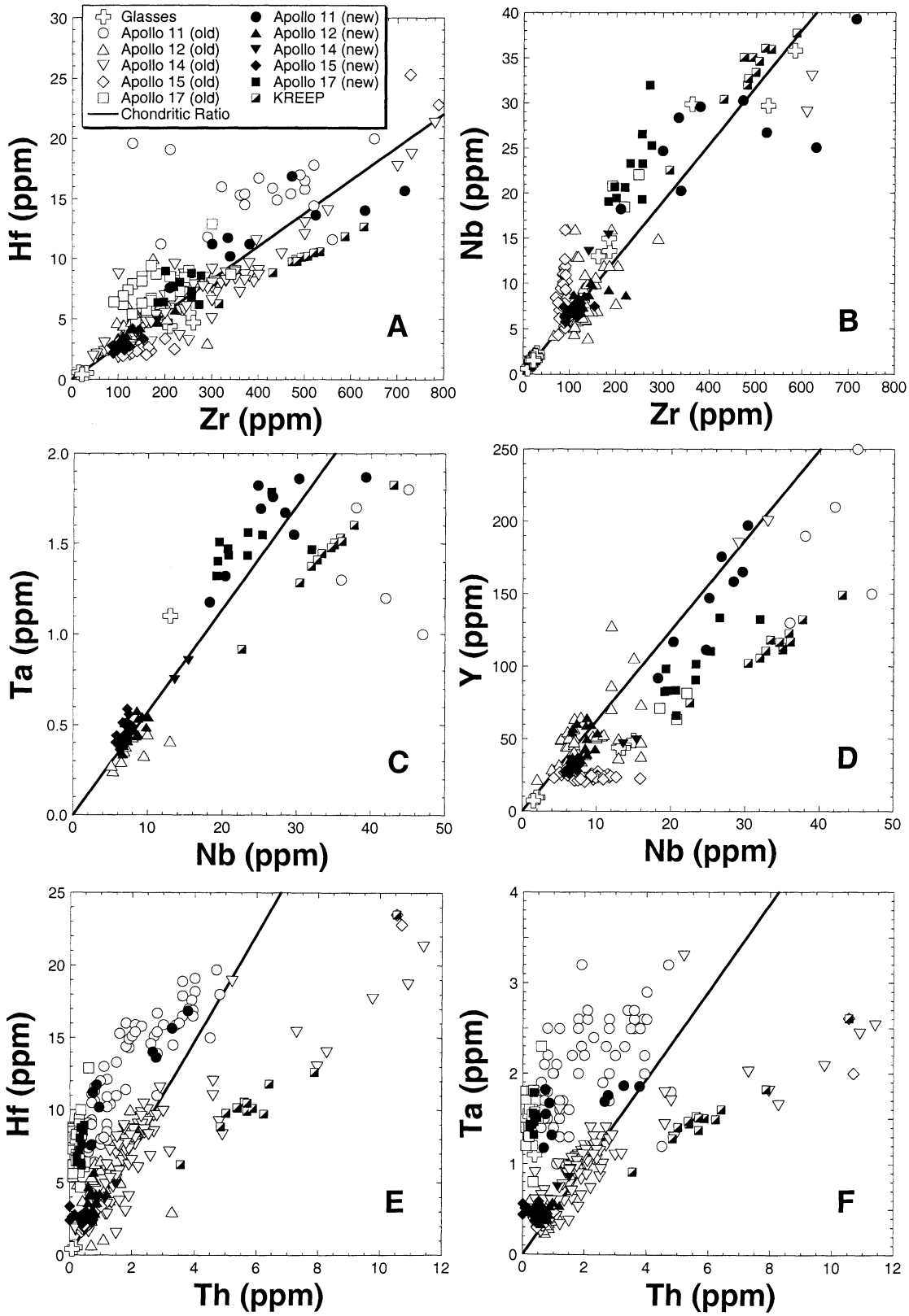

Figure 2. New ICP-MS data for the high field strength elements and Y from 63 mare basalts are compared with literature data for the basalts and KREEP (see *Neal and Taylor* [1992] for basalt data sources; KREEP compositions are from *McKay and Weill* [1976, 1977], *McKay et al.* [1978, 1979], and *Vaniman and Papike* [1980]). The solid line in each diagram represents the chondritic ratio (taken from *Sun and McDonough* [1989]).

low-Ti and Apollo 11 high-Ti basalts have approximately chondritic Nb/Y ratios However, Apollo 17 high-Ti basalts exhibit consistently suprachondritic values (Figure 2d), as do the KREEP samples. The new data dramatically reduce the range of Nb/Y ratios exhibited by the literature data for the low-Ti basalts (Figure 2d). There is a marked difference between Nb/Ta and Nb/Y ratios defined by the new ICP-MS data presented here for Apollo 11 basalts and literature data; the literature data giving suprachondritic Nb/Ta ratios (Figure 2c).

There are more literature data for Hf, Th, and Ta (Figures 2e and 2f) as these elements can be quantified by instrumental neutron activation. The new data are consistent with those in the literature in that the high-Ti basalts have suprachondritic Hf/Th ratios, whereas the low-Ti basalts have approximately chondritic ratios and KREEP exhibits subchondritic values (Figure 2e). A similar situation is seen with Ta/Th ratios (Figure 2f). Both Figures 2e and 2f demonstrate that igneous products containing a KREEP component will fall to the right of the chondritic line. Apollo 15 KREEP basalts [cf. *Vaniman and Papike*, 1977, 1980] and Apollo 14 high-Al basalts that have assimilated KREEP [*Neal et al.*, 1988a, 1988b, 1989] or contained KREEP in their source regions [*Dickinson et al.*, 1989] plot in these areas.

4. Discussion

4.1. Mare Basalt Sources

The new data presented above for the mare basalts are used in conjunction with literature data for the volcanic glass beads and the selected literature data to examine source region compositions. As seen above, the new basalt data exhibit generally chondritic HFSE (+Y) ratios (although exceptions do exist; Figure 2), even though the source regions have been processed by LMO crystallization. However, unlike the mantle of Earth, the lunar mantle has not experienced repeated processing after LMO crystallization, which would tend to emphasize the slight differences in HFSE mineral partition coefficients. KREEP generally exhibits nonchondritic ratios in Figure 2, probably as a result of Fe-Ti oxide addition or removal (see the complementary nature of the high-Ti basalts and KREEP in Figures 2e and 2f). Note that the Apollo 11 high-K (Group A) basalts plot at intermediate values to other high-Ti basalts and KREEP (Figures 2e and 2f). The new data simplify the picture of the mare basalt source regions as defined by HFSE ratios (+Y); they are consistent with overturn of the cumulate pile that added excess ilmenite into the low-Ti source and/or possibly a KREEP component (e.g., the Apollo 11 high-K or Group A basalts), thus disturbing a source region that had originally developed with chondritic HFSE (+Y) ratios.

4.2. Volcanic Glass Sources

There are significant compositional differences between the crystalline basalts and the glass beads. In terms of major elements, the volcanic glass compositions span the same range of TiO_2 contents as the basalts (Figure 3) and extend the upper range to >16 wt% TiO_2. Generally, the glasses contain greater amounts of MgO and FeO and lower abundances of Al_2O_3 and CaO compared to the basalts (Figures 3a-3d). *Delano* [1986] demonstrated that the volcanic glass groups he identified had generally experienced fractional crystallization, similar to the majority of the mare basalts. HFSEs (+Y) data available for the volcanic glasses suggest that the glass source was approximately chondritic for the ratios defined in Figure 2.

The glasses are usually more HREE-depleted relative to the basalts (Figure 4a). In addition, there appear to be two broad groups of glasses defined on the basis of depth of Eu anomaly and degree of HREE depletion. One population exhibits a relatively small negative Eu anomaly [$(Sm/Eu)_N$ = 1-2] with a moderate range in $(Sm/Yb)_N$ ratio (1-3) and REE abundances (Figures 4a-4c). The second population has a deeper Eu anomaly [$(Sm/Eu)_N$ = 1-9], a lower degree of LREE enrichment [$(Sm/Yb)_N$ = 1-2], and lower REE abundances (Figures 4a-4c). In the former group, REE contents are generally correlated with increasing TiO_2 contents but do not appear to be associated with KREEP (Figure 4c). The negative Eu anomaly exhibits little variation with Ti content (Figure 4d). The second glass population exhibits Eu anomalies akin to KREEP (Figure 4d). *Hughes et al.* [1988, 1989], *Hess* [2000], and *Shearer et al.* [1989, 1990, 1991, 1994, 1996a, 1996b] have used the trace element contents of the volcanic glasses to conclude that a mixed cumulate source is the most appropriate explanation for the source regions. These authors used high incompatible trace element contents and LREE/HREE ratios to demonstrate the incorporation of KREEP into the glass source region. This can explain the presence of the negative Eu anomaly in the glasses. However, this anomaly can also be generated by assimilation. *Elkins et al.* [2000] showed, though high-pressure experimental studies, that the Apollo 14B green glass could be generated by a low-Ti magma of first a high-Ti cumulate followed by a KREEP component. This alternative is explored below.

4.3. Assimilation Model: Evidence from Glass Compositions

The persistent negative Eu anomaly in the volcanic glasses is generally smaller than in the basalts (Figure 4). However, its very presence has been interpreted to suggest that the glasses are derived from lunar magma ocean (LMO) cumulate material derived from a liquid that had experienced plagioclase removal [e.g., *Taylor and Jâkes*, 1974; *Snyder et al.*, 1992; *Shearer and Papike*, 1993, 1999]. As noted above, while experimental petrology suggests that the glasses were derived from deeper levels in the lunar mantle, there is some ambiguity over the results. *Shearer and Papike* [1999] have suggested that the glasses and basalts could have been produced under the same pressure but in a laterally heterogeneous mantle. The presence of the small, persistent negative Eu anomaly appears to argue against derivation from a source that escaped the LMO melting event.

The alternative suggested here is that polybaric fusion [e.g., *Longhi*, 1992; *Wagner and Grove*, 1997] coupled with sequential assimilation [e.g., *Elkins et al.*, 2000] can produce the range in volcanic glass compositions. It is assumed that the source is represented by a bulk Moon composition [*Taylor*, 1990] containing approximately chondritic ratios of the REE and HFSEs. Using Nb/Ce, Nb/Zr, and $(Sm/Eu)_N$ ratios, the feasibility of generating the glass compositions by assimilating ilmenite-rich cumulates is demonstrated (Figure 5). Three simple models are presented using bulk mixing. Model 1 involves a melt derived from a bulk Moon source assimilating ilmenite. Model 2 uses an 80:20 mixture of ilmenite and KREEP (trapped melt, which is taken to be LKFM [*McKay et al.*, 1978; *Vaniman and Papike*, 1980]). Model 3 uses a 50:50 mixture of ilmenite and KREEP as the assimilant. Abundances of Nb, Zr, Sm, and Eu in ilmenite were calculated using the *McCallum and Charette* [1978] and *McKay et al.* [1986] partition coefficients, assuming ilmenite crystallized from

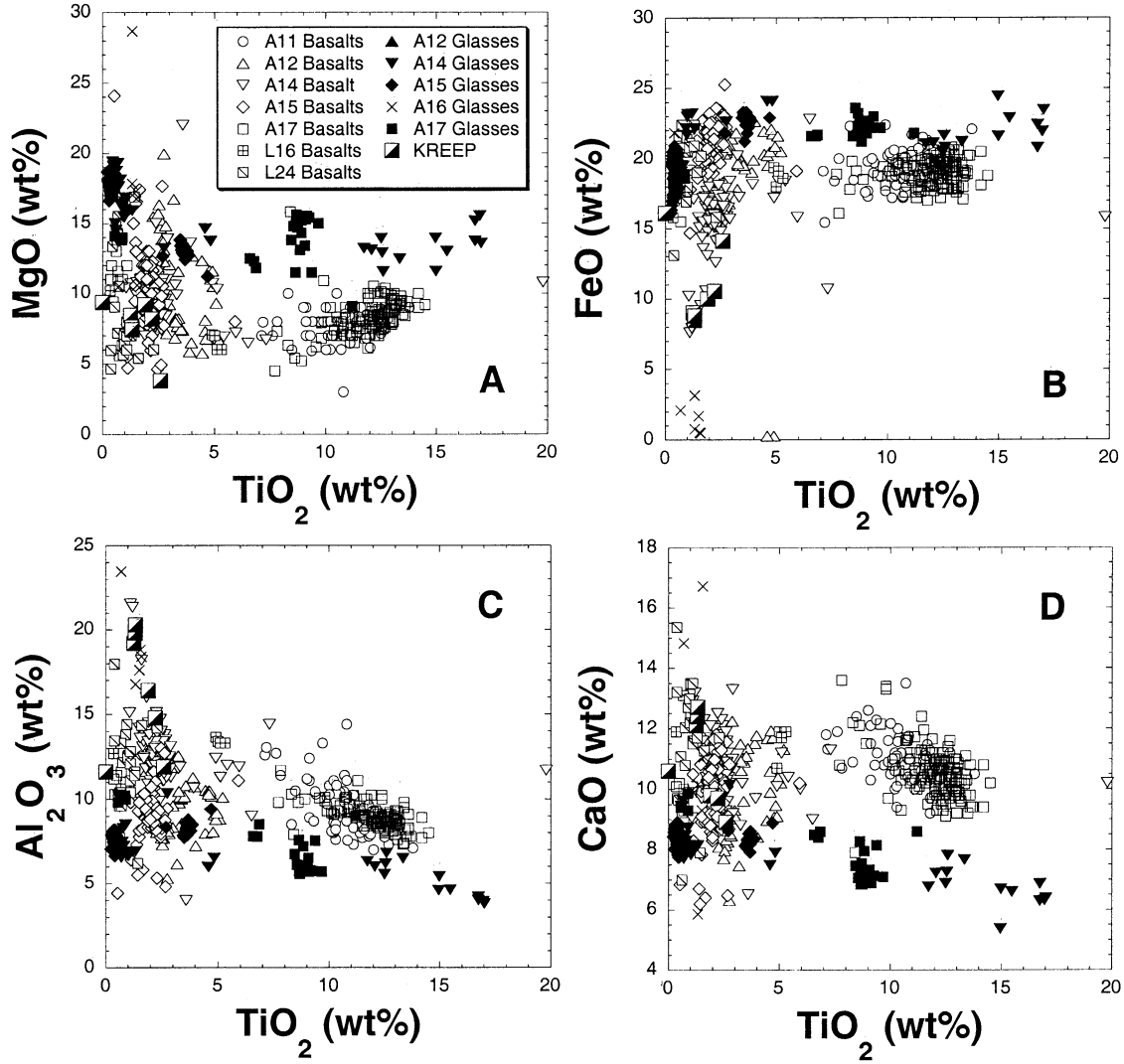

Figure 3. Comparison of major element compositions between mare basalts and volcanic glass beads (see *Neal and Taylor* [1992] for basalt data sources; glass data from *Shearer et al.* [1989, 1990, 1991, 1994, 1996a, 1996b], *Hughes et al.* [1988, 1989], *Delano* [1986], *Delano and Livi* [1981], and *Steele et al.* [1992]; KREEP compositions are from *McKay and Weill* [1976, 1977], *McKay et al.* [1978, 1979], and *Vaniman and Papike* [1980]).

KREEP. It is evident that the mixed assimilants Models 2 and 3 can generate observed glass compositions. However, the position of the KREEP field in Figures 5a-5c shows that initial ilmenite assimilation (Model 1) followed by KREEP assimilation (vectors off the ilmenite mixing trend toward the KREEP field defined by data from McKay *and Weill* [1976, 1977], *McKay et al.* [1978, 1979], and *Vaniman and Papike* [1980]) is more effective in generating the volcanic glasses. This is most striking for TiO_2 versus $(Sm/Eu)_N$ (Figure 5c), where the glass data plot above from the horizontal Model 1 toward KREEP.

Longhi [1992] suggested that melting may have been initiated as deep as 1000 km for the very low Ti volcanic glasses. If this is the case, the range of Ti contents of the glasses (Figures 4c, 4d, and 5) could be generated by initial assimilation of ilmenite-rich cumulates that sank to the base of the magma ocean cumulate pile [*Hubbard and Minear*, 1976; *Wagner and Grove*, 1993, 1995, 1997; *Elkins et al.*, 2000]. This would account for the range in TiO_2 contents of the glasses and impart a slight negative Eu to the glass magma (according to crystal liquid partition coefficients of *McKay et al.* [1986]), owing to the fact that ilmenite would have been crystallized from the LMO after plagioclase [cf. *Snyder et al.*, 1992]. In Figure 6, the vector defining the compositional evolution of parental glass magmas generated in a bulk Moon (VLT) source region beneath the LMO cumulate pile is plotted as it assimilates ilmenite-rich cumulates at the base of the LMO. If the magma continued to rise, undergoing polybaric melting [e.g., Longhi, 1992], it is feasible that KREEP-rich materials, which would contain high concentrations of heat-producing elements and would therefore be hot, could subsequently be assimilated.

In a simple bulk mixing model, $(Eu/Eu^*)_N$ values have been calculated for the volcanic glasses by extrapolation of chondrite-normalized La, Ce, and Sm values through Eu. Four potential "parents" were used from the literature data with $(Eu/Eu^*)_N$ close to unity (i.e., small to no negative Eu anomaly), and with TiO_2 contents reflecting the range of glass compositions in Figure 3, ranging from VLT (<1 wt% TiO_2) to high-Ti (>10 wt.% TiO_2). These parental compositions plot on or close to the vector for

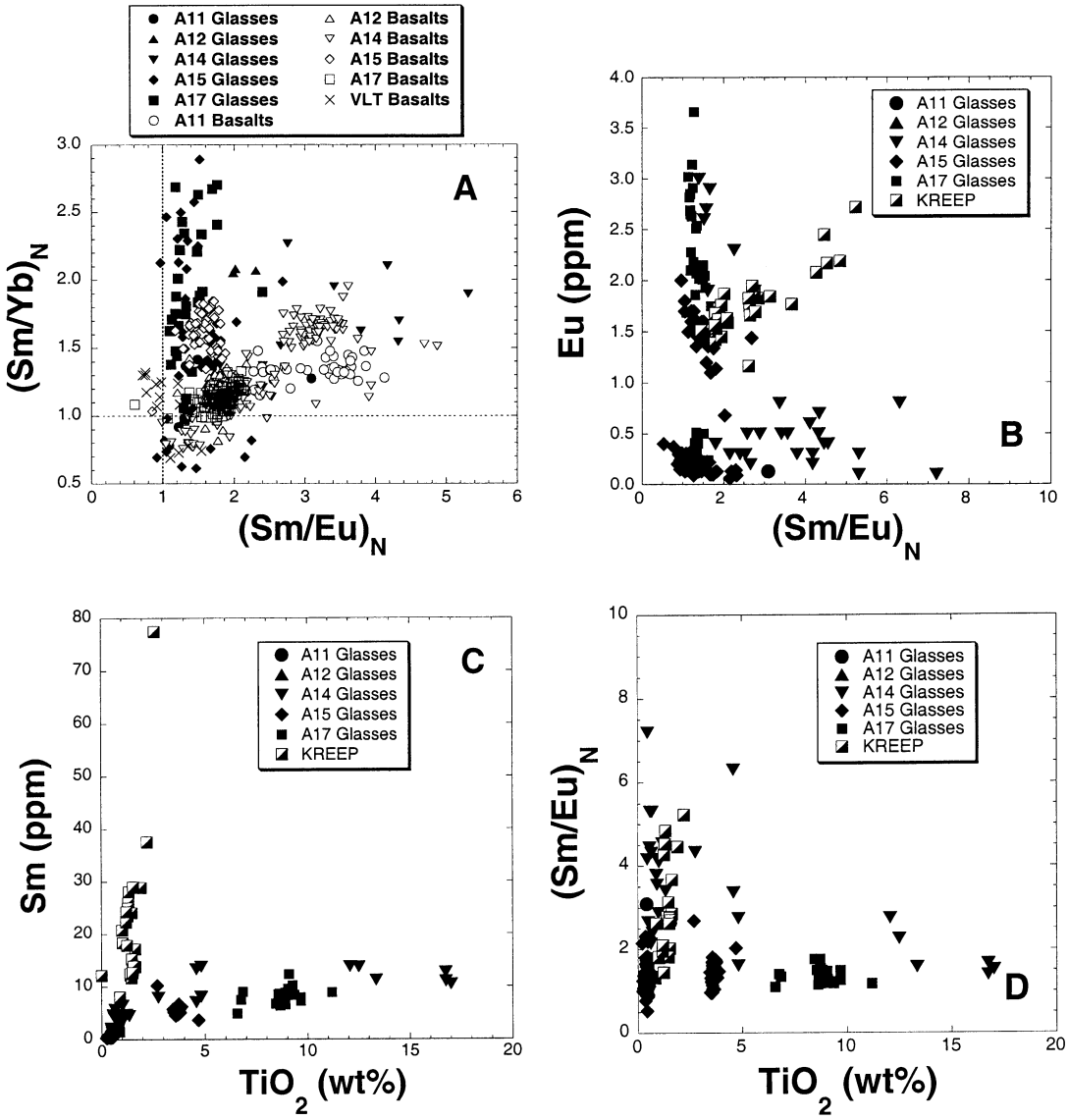

Figure 4. Rare earth element and TiO_2 systematics for the volcanic glass beads. Data sources are as in Figure 3. This figure demonstrates the presence of a small negative Eu anomaly in the glasses and shows that increased LREE enrichment is a function of TiO_2 content in the glasses. Figure 4a compares the slope of the REE profile with the depth of the negative Eu anomaly between the volcanic glasses and the mare basalts. Figures 4b-4d depict only the glass compositions as a function of landing site. Subscript N represents chondrite normalized ratios.

initial ilmenite assimilation (Figure 6). The KREEP component used was an average KREEP composition (data from *McKay and Weill* [1976, 1977], *McKay et al.* [1978, 1979], and *Vaniman and Papike* [1980]). Rare earth element contents increase with Ti content, so the amount of mixing was increased incrementally with the length of the lines from each parent representing 10%, 20%, 30%, and 40% with increasing TiO_2 (Figure 6).

It is evident that simple bulk assimilation by a hot, picritic melt of an ilmenite-rich cumulate followed by a KREEP component can account for the presence of the persistent negative Eu anomaly in the volcanic glasses, as well as the range in TiO_2 contents [cf. *Wagner and Grove*, 1993, 1995, 1997; *Elkins et al.*, 2000]. It is suggested that assimilation is a viable alternative to the mixed source (cumulate overturn) model, especially as the KREEP component would be relatively enriched in heat-producing elements, thus making it easier to assimilate.

4.4. Evidence of Garnet in the Source of Some Volcanic Glasses

The assimilation model requires that at least some glass source regions lie below the LMO cumulates and would therefore be in a region of the Moon where garnet is stable. The influence of garnet on magmatic compositions will be most dramatic on the heavy REE and Y if garnet is not exhausted by the melting event(s) and is retained in the residue. This would result in elevated element/HREE or element/Y ratios. Assimilation of late stage cumulate and KREEPy materials to produce the high-Ti contents of some glasses and the ubiquitous negative Eu anomaly

would also impart elevated values for these ratios. Therefore careful examination of the data is required to delineate between these two mechanisms, especially as KREEP involvement is required both in the mixed source models for glass petrogenesis

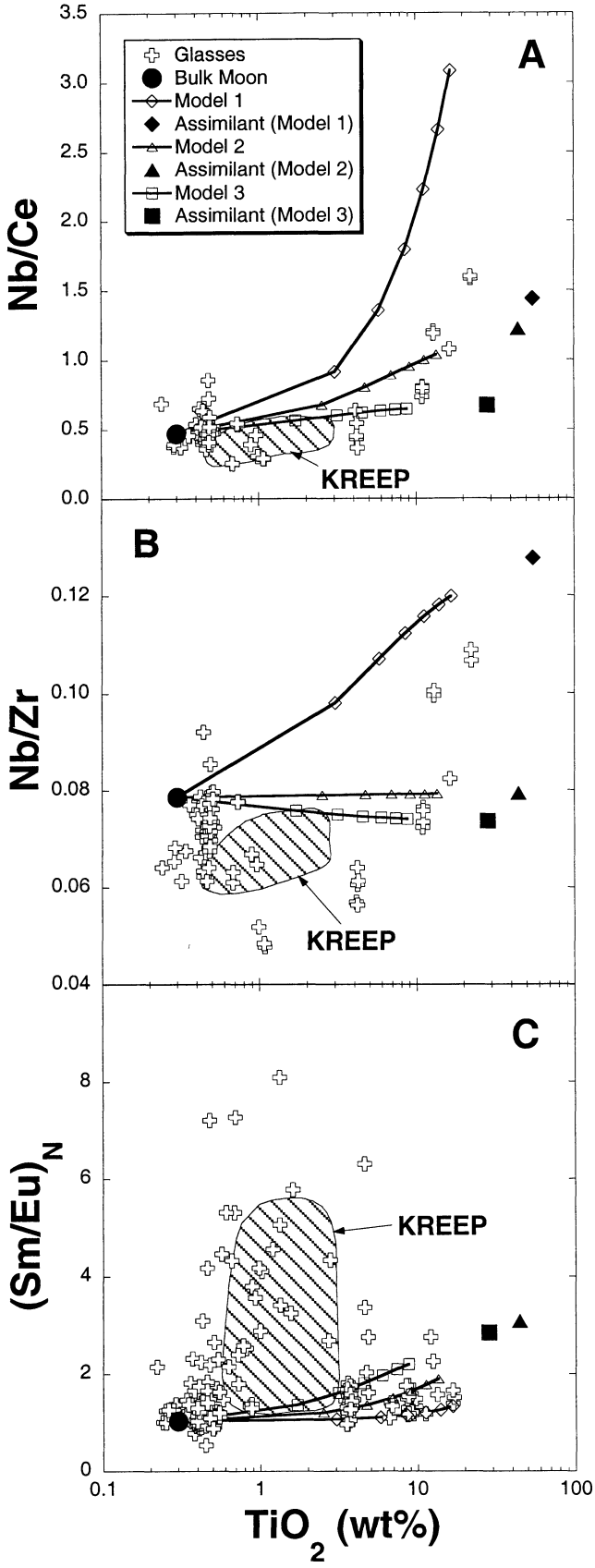

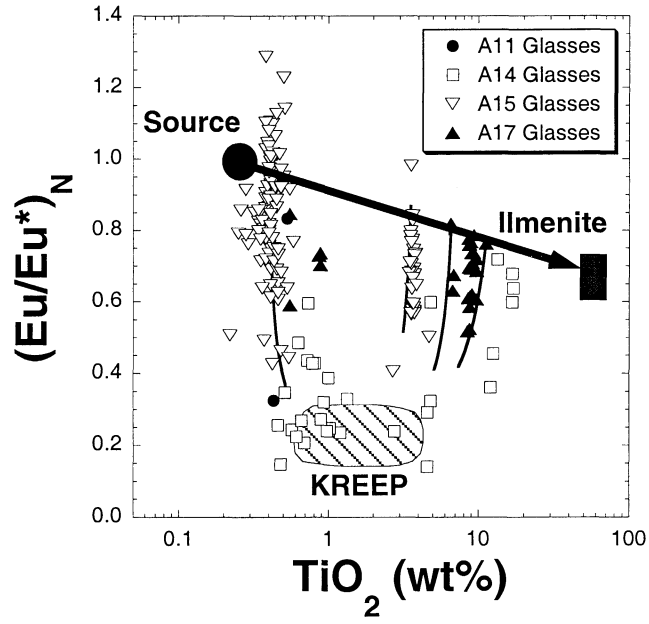

Figure 6. Modeling of the proposed sequential assimilation to produce the range of TiO_2 contents of and ubiquitous negative Eu anomaly in volcanic glasses. Data sources are as in Figure 3. A VLT/low-Ti parental magma with no Eu anomaly (solid circle) initially assimilates ilmenite (solid rectangle) following the vector indicated by the arrow. Bulk mixing trends between actual glass compositions (representing VLT, low-Ti, intermediate-Ti, and high-Ti groups) along this vector and KREEP are calculated. Data sources for KREEP are as in Figure 2 and for the glasses as in Figure 3. The mixing trajectories extending toward the KREEP field represent (from right to left) 10%, 20%, 30%, and 40%, respectively, KREEP assimilation by the parental magma composition. See text for discussion.

[e.g., Shearer *et al.*, 1991, 1994, 1996a, 1996b] and in the assimilation model (see above and Figure 6).

Examination of compositional differences between mare basalts and volcanic glasses shows that the basalts generally exhibit chondritic Zr/Y and Zr/Yb ratios (Figures 7a and 7b), although the Apollo 11 high-K and Apollo 14 basalts tend to exhibit suprachondritic Zr/Yb probably owing to the influence of KREEP (see above). The volcanic glasses contain suprachondritic values for both Zr/Y and Zr/Yb, similar to KREEP (Figures 7a and 7b) and would be consistent with not only the mixed cumulate source hypothesis [e.g., *Shearer and Papike*, 1993; *Hess*, 2000], but also the assimilation model [*Hubbard and Minear*, 1976; *Wagner and Grove*, 1997; *Elkins et al.*, 2000] (see

Figure 5. Illustrations demonstrating the feasibility of ilmenite assimilation by a VLT/low-Ti parent magma derived from a bulk Moon source for generating the range of volcanic glass compositions. Ilmenite is plotted using average mineral data (TiO_2) and using the partition coefficients of *McCallum and Charette* [1978] and *McKay et al.* [1986] for the (A) Nb/Ce, (B) Nb/Zr, and (C) $(Sm/Eu)_N$ ratios (the assimilant composition for Model 1 is not shown in this panel as it has an extremely high $(Sm/Eu)_N$ ratio of ~ 250). Data sources are as in Figure 3. Symbols on the model trajectories represent progressive mixing of the assimilant in 5% increments. The assimilant for Model 1 is ilmenite crystallized from a LKFM KREEP liquid. For Model 2 the assimilant is an 80:20 mixture of ilmenite and LKFM KREEP, and for Model 3 the assimilant is a 50:50 mixture of these components.

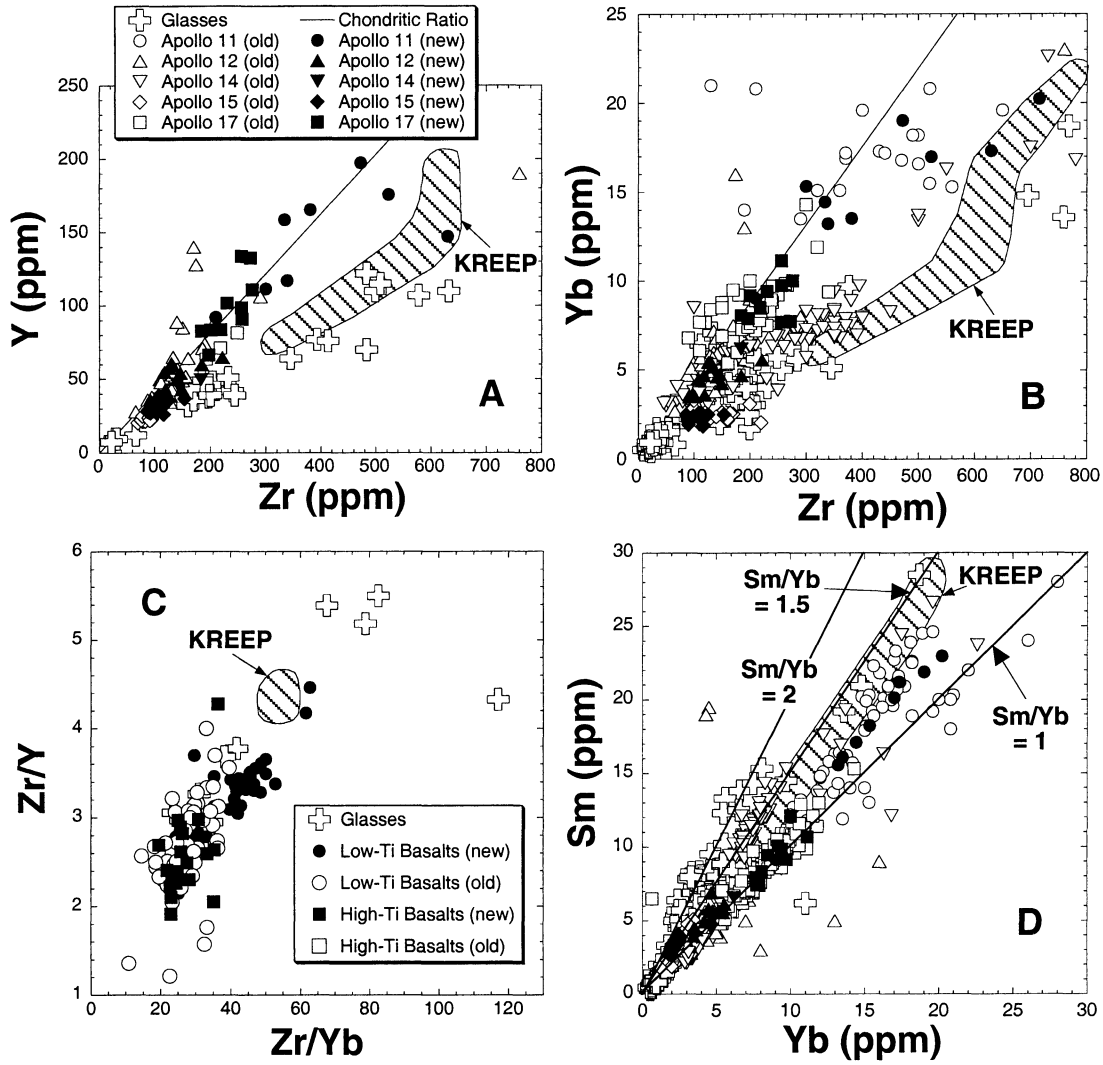

Figure 7. Diagrams illustrating the role of garnet in the source regions of some of the volcanic glasses. Symbols defined in Figure 7a are also used in Figures 7b and 7d. Data sources are as in Figure 3. See text for discussion.

above). However, *Neal* [1998, 1999] interpreted these relationships as an indication of garnet retention in the source residue of at least some volcanic glasses. Although the database is small, there are clear distinctions between mare basalt, KREEP, and glass Zr/Y and Zr/Yb ratios. The mare basalts and some glasses have Zr/Y ratios <4 and Zr/Yb ratios <50, KREEP forms a tight group with Zr/Y ~ 4.5 and Zr/Yb ~ 57, whereas some volcanic glasses have ratios in excess of the KREEP values (Figure 7c). Clearly, not all the volcanic glass compositions can be explained by simple KREEP involvement. This is further emphasized when the slope of the REE profiles is considered. Some volcanic glasses exhibit the steepest slope (highest Sm/Yb ratio of ~ 2), whereas the mare basalts and remaining glasses display Sm/Yb ratios of between 1 and 1.25, with KREEP being intermediate (~ 1.5; Figure 7d). It is the glasses with Sm/Yb ratios greater than KREEP that are evidence that garnet was a residual component after the cessation of partial melting.

The presence of garnet in the lunar mantle has been proposed by several authors using interpretations of seismic data [e.g., *Anderson*, 1975; *Hood*, 1986; *Hood and Jones*, 1987]. However, interpretations based on the limited seismic data are ambiguous. For example, *Nakamura et al.* [1974] and *Nakamura* [1983] suggested that higher velocities in the middle mantle (>500 km) could be indicative of an increased proportion of Mg-rich olivine. What has become apparent is a seismic discontinuity around 500 km, albeit somewhat heterogeneous in nature [*Kahn et al.*, 2000] and this has been interpreted as the maximum depth of LMO melting [*Goins et al.*, 1981; Nakamura, 1983; *Mueller et al.*, 1988; *Hood and Zueber*, 2000]. *Kuskov and Fabrichnaya* [1994], *Kuskov* [1995, 1997], and *Kuskov and Kronrod* [1998] calculated the stable phases in compositional models, along with their respective seismic properties, using the method of minimization of Gibbs free energy. The models were then compared with the seismic observations for the lunar interior. The results of the studies by Kuskov and coworkers suggest that garnet (<1 mol %) would be a stable (albeit minor) phase in the middle mantle of the Moon between 270 and 500 km, but would be a significant phase in the lower lunar mantle between 500 and 1262 km (8-13 mol %).

The significance of these observations and model results is that they demonstrate the potential for garnet to be a stable phase in the lunar mantle. *Beard et al.* [1998] suggested that garnet may have been in the source region of the low-Ti mare basalts on the basis of Lu-Hf isotope systematics. They argued that

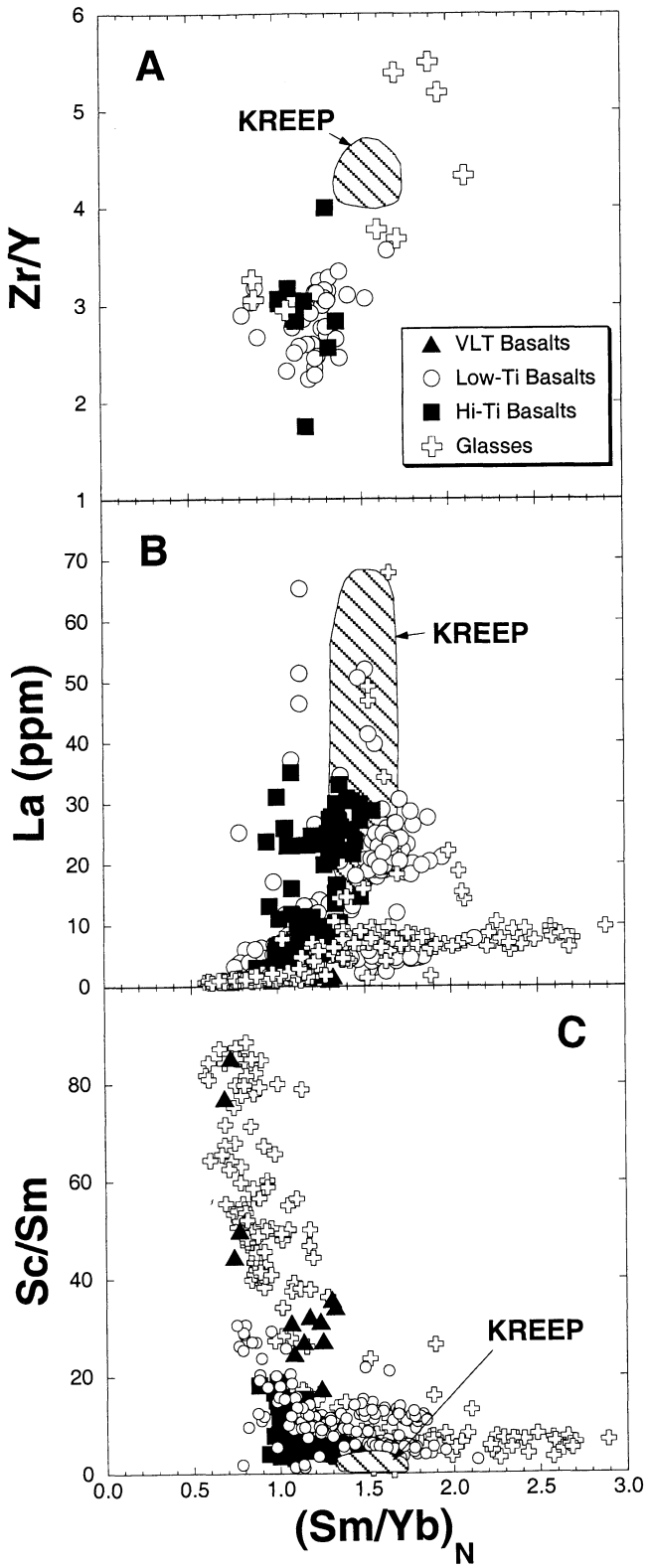

Figure 8. These plots illustrate that some glass compositions cannot be generated by the addition of KREEP, although others clearly contain a KREEP signature. Data sources are as in Figure 3. See text for discussion.

orthopyroxene and garnet are the only phases capable of producing the required large fractionations of Lu/Hf and Sm/Nd in the mare basalt source. Garnet was relegated to background significance because it was recognized that it did not directly crystallize from the LMO [cf. *Snyder et al.*, 1992; *Beard et al.*, 1998]. However, it may have stabilized in the lowermost portions of the cumulate pile through metamorphic transformations as the LMO cumulates stabilized and cooled. The sinking of ilmenite-rich cumulates to the lowermost reaches of the cumulate pile would introduce heterogeneity in the mare basalt source region, producing high- and low-Ti basalts from a potentially garnet-bearing source. However, no evidence of garnet retention is the source of the mare basalts is seen in other trace element data (Figures 7 and 8). If garnet was ever present in the mare basalt source, it was probably exhausted during partial melting. The preferred model of *Beard et al.* [1998], which required orthopyroxene-rich source regions and low degrees of partial melting to satisfy Lu-Hf and Sm-Nd isotopic systematics, is supported by the mare basalt trace element data.

It is recognized that not all glass compositions exhibit evidence for garnet in their source regions. For example, the slope of the REE profile and REE abundances illustrate that at least a proportion of volcanic glasses has been affected by KREEP (Figures 7 and 8). However, a significant number of the volcanic glasses have LREE-enriched profiles above what would be expected by KREEP involvement, either in the source or through assimilation (Figures 8a-8c). For example, these glasses have elevated $(Sm/Yb)_N$ and Zr/Y ratios above those of KREEP (Figure 8a) but have relatively low REE abundances (Figure 8b). In addition, garnet retention in the source would have a dramatic effect on the abundance of Sc in the resultant melts, which would result in lower values for ratios such as Sc/Sm. Volcanic glasses with low Sc/Sm ratios also have elevated values for $(Sm/Yb)_N$ (Figure 8c). It is these glasses (Apollo 12 red, Apollo 14 green A and yellow, and Apollo 17 orange type I and 74220-type) that I conclude were derived from a garnet-bearing source. Using the results of *Kuskov and Fabrichnaya* [1994], and *Kuskov* [1995, 1997], garnet would be more prevalent in the lunar lower mantle (>500 km), resulting in a likely scenario of garnet being retained in the residue after the partial melting that produced parent magmas for the volcanic glasses.

Nonmodal batch melting of a bulk Moon composition has been modeled using a garnet-bearing (solid line and solid diamonds in Figure 9) and garnet-free source (dashed line and open diamonds in Figure 9). The former is taken to represent peridotite (50% olivine, 25% orthopyroxene, 20% clinopyroxene, and 5% garnet melting in the proportions of 15:25:40:20). The latter is taken as a mixed cumulate source (50% olivine, 30% orthopyroxene, 15% clinopyroxene, 5% ilmenite melting in the proportions 15:25:40:20). Both sources are assumed to have a bulk Moon composition [cf. *Taylor*, 1982, 1990] and partition coefficients are taken from the compilations in *Snyder et al.* [1992] and *Green* [1994] (basaltic compositions). Results indicate that the mixed cumulate (garnet-free) source cannot generate the $(Sm/Yb)_N$ and Zr/Y ratios observed in the volcanic glasses; a garnet-bearing source is required (Figure 9a). When REE abundances are modeled (represented here by La), garnet is required to be retained in the melt residue in order to account for the high $(Sm/Yb)_N$ ratios for the relatively low La abundances (Figure 9b). Approximate degrees of partial melting are between 10 and 25%.

The volcanic glasses define a wide range of values for the Sc/Sm ratio (Figures 8c and 9c). The bulk Moon source used in the model plots approximately in the middle of this range. Both the garnet-bearing and garnet-free sources produce melts of lower Sc/Sm ratio than the source, although the garnet-bearing source is the only one that produces melts that also contain higher $(Sm/Yb)_N$ ratios, as required by the glasses that plot in the lower right of Figure 9c. Melting of this bulk Moon source cannot pro-

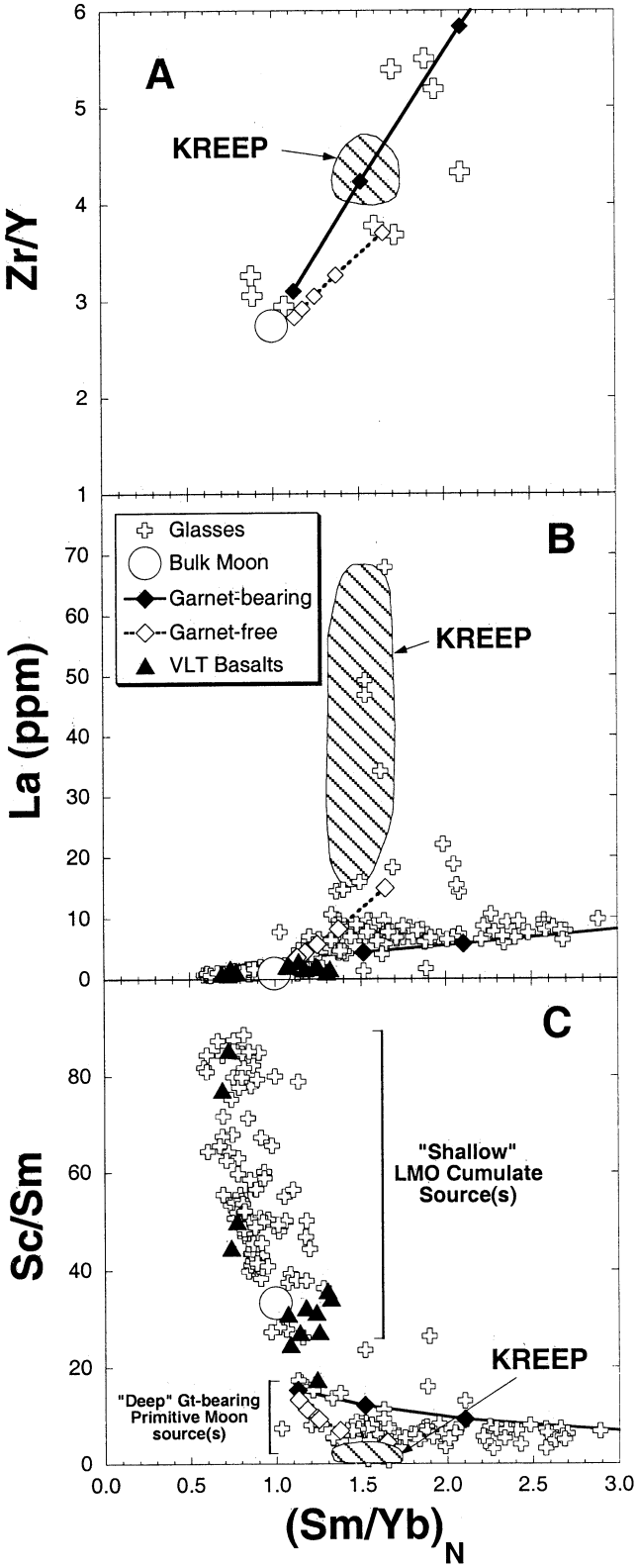

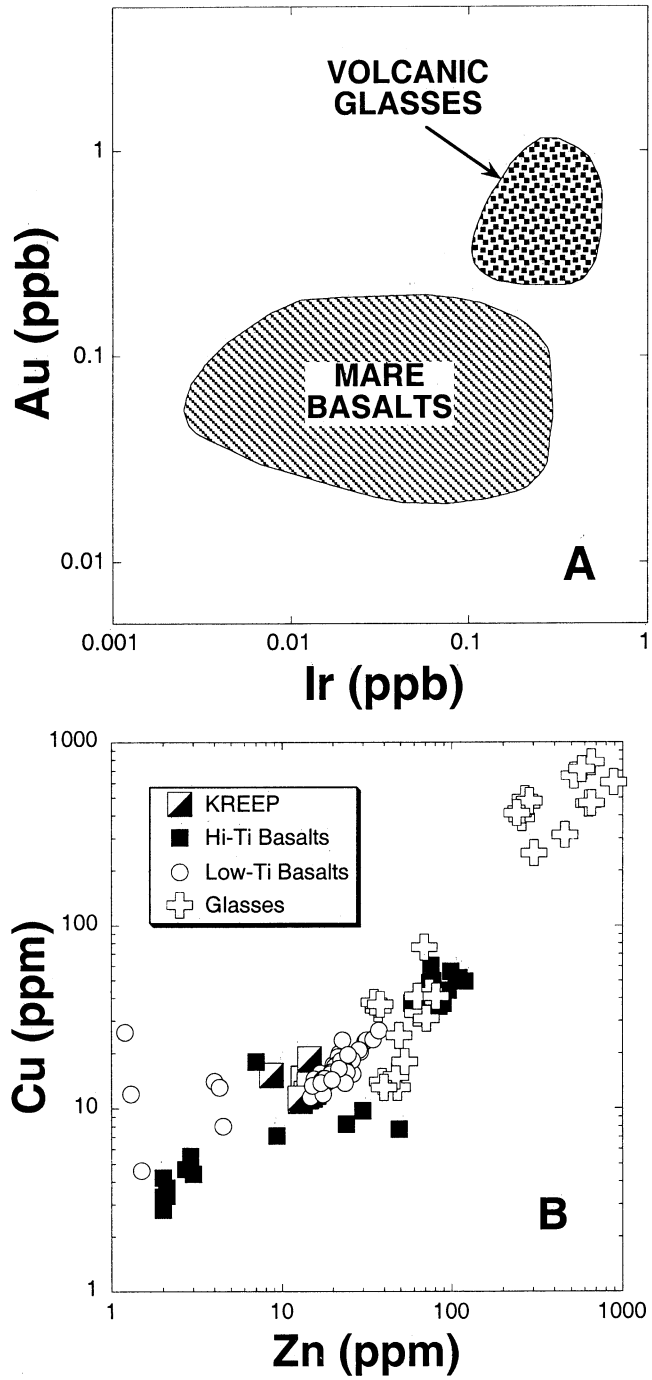

Figure 10. Siderophile and chalcophile element data for the mare basalts, volcanic glasses, and KREEP [Shearer et al., 1989, 1990, 1991, 1994, 1996a, 1996b; Anders et al., 1971; Morgan et al., 1972a, 1972b, 1974; Ganapathy et al., 1973; this study]. See text for discussion.

Figure 9. These plots illustrate the effects of retaining garnet in the residue after partial melting. Dashed lines and open diamonds represent a garnet-free source, and solid lines and solid diamonds represent a garnet-bearing source. The symbol on the melt line closest to the source composition represents 25% partial melting. Subsequent symbols moving away from the source represent a 5% decrease in partial melting. Bulk Moon is taken from *Taylor* [1990], and the data sources are as in Figure 3. See text for discussion.

duce the glasses containing higher Sc/Sm ratios than bulk Moon. Significantly, the VLT basalts of Apollo 17 and Lunar 24 span the range of Sc/Sm and $(Sm/Yb)_N$ ratios of this group of glasses (Figure 9c), which are all VLT. Therefore this group of glasses is interpreted to have been derived from early (olivine and orthopyroxene, no ilmenite) LMO cumulates and melts from such a source assimilated varying proportions of KREEP on the way to the surface. The second group of volcanic glasses (lower right, Figure 9c) are interpreted as having been derived from a garnet-

bearing, bulk Moon source that escaped the LMO melting event (see below). These melts assimilated varying proportions of ilmenite-rich (late stage) cumulates and KREEP as they ascended to the surface.

Why, then, do multiple-saturation experiments on the volcanic glasses not demonstrate the existence of garnet in the source [e.g., *Green et al.*, 1975; *Delano*, 1980]? This could be because the glasses are formed by polybaric melting, initiated at ~ 1000 km and ceasing at 100 km [*Longhi*, 1992; *Wagner and Grove*, 1997]. Multiple-saturation experiments would give an average pressure, possibly outside the garnet stability field. Alternatively, the shallower-level assimilation processes could affect the multiple-saturation experiments, masking the garnet signature in some of these glasses. Finally, the glass compositions used in the multiple saturation experiments were not the ones derived from a garnet-bearing source.

4.5. Primitive Moon or Garnet-Bearing LMO Cumulate?

Geophysics, thermodynamic modeling, and geochemistry appear to be arriving at a consensus that garnet is present in the deep lunar interior. The lunar magma ocean processed only the outer ~500 km of the Moon, leaving the interior untouched. This garnet-bearing "primitive" Moon became the source region for at least some of the volcanic glasses. If this is correct, it would be expected that siderophile and chalcophile elements (e.g., Ir, Au, Cu, and Zn) would be elevated in this region for two reasons. The first is that siderophile and chalcophile elements were not as efficiently scavenged from the primitive Moon during the formation of the small lunar core [cf. *Hood et al.*, 1999] as they were from the LMO. Second, the siderophile and chalcophile elements scavenged (efficiently) from the LMO would have to permeate (inefficiently) through the relative solid primitive interior of the Moon. Therefore the volcanic glasses derived from a primitive Moon source should contain higher siderophile and chalcophile element abundances relative to the crystalline basalts. Simple elemental relationships seem to confirm this (Figures 10a and 10b). Although the database is not extensive, the glasses for which data are available [*Anders et al.*, 1971; *Morgan et al.*, 1972a and 1972b, 1974; *Ganapathy et al.*, 1973] have generally higher Ir and Au abundances relative to the basalts (Figure 10a). Perhaps most significantly, the Cu and Zn data demonstrate that there are two groups of glasses. One group has abundances greater than the basalts, and the other has abundances comparable to the mare basalts (Figure 10b). The former group contains glasses with $(Sm/Yb)_N$ >1.5, and it is concluded that they were derived from a garnet-bearing, primitive Moon source. The latter group contains glasses with lower $(Sm/Yb)_N$ (<1.5) and higher Sc/Sm ratios (>30), and it is concluded that they were derived from a garnet-free source region in the LMO cumulate pile similar to the mare basalts.

5. Conclusions

The mare basalt compositions reported here demonstrate that they were derived from LMO cumulate source regions. The new data suggest that despite processing via the magma ocean, the source regions contained generally chondritic HFSE ratios. The high-Ti basalts deviate from this generalization and this can be explained by addition of late stage ilmenite through overturn of the cumulate pile or sinking of the dense late stage cumulates. The influence of KREEP is seen in the Apollo 11 "high-K" (Group A) and in some Apollo 14 basalts.

A significant subset of the volcanic glasses was derived from source regions that contained garnet that was retained in the residue. This resulted in magmas with LREE-enriched profiles greater than KREEP but relatively low trace element contents. It is evident that some glass compositions have been influenced by incorporation of KREEP and others have relatively flat REE profiles. The latter are probably melt products of a VLT source region that is dominated by early LMO cumulates (olivine-orthopyroxene). Therefore the compositions of the lunar volcanic glass beads represent derivation from both garnet-bearing and garnet-free sources with variable incorporation of a KREEP component. Those derived from garnet-bearing sources are enriched (relative to the mare basalts) in siderophile and chalcophile elements (Figures 10a and 10b). This is interpreted as indicating that the source was not melted by the LMO event and represents "primitive Moon." Such enrichment could be generated by inefficient scavenging of these elements during core formation, as would be expected in a portion of the Moon that escaped melting during the LMO event. While the slope of the REE profile was generated in the source, the range in TiO_2 contents and negative Eu anomaly were incorporated through sequential assimilation, first of a dense ilmenite-rich cumulate (probably near the base of the LMO) followed by assimilation of a KREEP component [cf. *Elkins et al.*, 2000]. This sequential assimilation would certainly be possible if polybaric partial fusion is the mechanism for melt generation. The fact that the glasses with the high-Ti signature also appear to have been generated beneath the LMO cumulate pile in the garnet-bearing primitive Moon suggests that the magma would have enough thermal energy to facilitate assimilation.

Acknowledgments. Jennifer Ryan, James Seidler, and Jinesh C. Jain are thanked for help with the ICP-MS analyses. The manuscript greatly benefited from a thorough review by Scott Hughes. This work was supported by NASA grant NAG5-8099.

References

Anders, E., R. Ganapathy, R.R. Keays, J.C. Laul, and J.W. Morgan, Volatile and siderophile elements in lunar rocks: Comparison with terrestrial and meteoritic basalts, *Proc. Lunar Sci. Conf. 2nd*, 1021-1036, 1971.

Anderson, D.L., On the composition of the lunar interior, *J. Geophys. Res., 80*, 1555-1557, 1975.

Beard, B.L., L.A. Taylor, E.E. Scherer, C.M. Johnson, and G.A. Snyder, The source region and melting mineralogy of high-titanium and low-titanium lunar basalts deduced from Lu-Hf isotope data, *Geochim. Cosmochim. Acta 62*, 525-544, 1998.

Cameron, A.G.W., The impact theory for the origin of the Moon, in *Origin of the Moon,* edited by W.K. Hartmann, R.J. Phillips, and G.J. Taylor, pp. 609-616, Lunar and Planet. Inst., Houston, Tex., 1986.

Cameron, A.G.W., and W. Benz, The origin of the Moon and the single impact hypothesis IV. *Icarus 126*, 126-137, 1991.

Cameron, A.G.W., and R.M. Canup, The giant impact and the formation of the Moon, paper presented at *Origin of Earth and Moon Conference,* Lunar and Planet. Inst., Monterey, Calif., 1998.

Cameron, A.G.W., and W.R. Ward, Origin of the Moon (abstract), *Lunar Sci. VII*, 120-122, 1976.

Chyi, L.L., and W.D. Ehmann, Zirconium and hafnium abundances in some lunar materials and implications of their ratios, *Proc. Lunar Sci. Conf. 4th*, 1219-1226, 1973.

Delano, J.W., Chemistry and liquidus phase relations of Apollo 15 red glass: Implications for the deep lunar interior, *Proc. Lunar Planet. Sci. Conf. 11th*, 251-288, 1980.

Delano, J.W., Pristine lunar glasses: Criteria, data, and implications, *Proc. Lunar Planet. Sci. Conf. 16th, Part 2 J. Geophys. Res., 91*, suppl. D201-D213, 1986.

Delano, J.W., Pristine mare glasses and mare basalts: Evidence for a general dichotomy of source regions, in *Workshop on Lunar Volcanic*

Glasses: Scientific and Resource Potential (edited by J.W. Delano and G.H. Heiken), pp. 30-31, *LPI Tech. Rep. 90-02*, Lunar and Planet. Inst., Houston, Tex., 1990.

Delano, J.W. and K. Livi, Lunar volcanic glasses and their constraints on mare petrogenesis. *Geochim. Cosmochim. Acta, 45*, 2137-2149, 1981.

Dickinson, T., G.J. Taylor, K. Keil, and R.W. Bild, Germanium abundances in lunar basalts: Evidence of mantle metasomatism, *Proc. Lunar Planet. Sci. Conf. 19th*, 189-198, 1989.

Duncan, A.R., A.J. Erlank, J.P. Willis, M.K. Sher, and L.H. Ahrens, Trace element evidence for a two-stage origin of some titaniferous mare basalts, *Proc. Lunar Sci. Conf. 5th*, 1147-1157, 1974.

Dungan, M.A. and R.W. Brown, The petrology of the Apollo 12 ilmenite basalt suite, *Proc. Lunar Sci. Conf. 8th*, 1339-1381, 1977.

Ehmann, W.D., L.L. Chyi, A.N. Garg, B.R. Hawke, M.-S. Ma, M.D. Miller, W.D. James, and R.A. Pacer, Chemical studies of the lunar regolith with emphasis on Zr and Hf, *Proc. Lunar Sci. Conf. 6th*, 1351-1361, 1975.

Elkins, L.T., V.A. Fernandes, J.W. Delano, and T.L. Grove, Origin of lunar ultramafic green glasses: Constraints from phase equilibrium studies, *Geochim. Cosmochim. Acta, 64*, 2339-2350, 2000.

Galbreath, K.C., C.K. Shearer, J.J. Papike, and N. Shimizu, Inter- and intra-group compositional variations in Apollo 15 pyroclastic green glass: An electron- and ion-microprobe study., *Geochim. Cosmochim. Acta, 54*, 2565-2575, 1990.

Ganapathy, R., J.W. Morgan, U. Krähennbühl, and E. Anders, Ancient meteoritic components in lunar highland rocks: Clues from trace elements in Apollo 15 and 16 samples, *Proc. Lunar Sci. Conf. 4th*, 1239-1261, 1973.

Garg, A.N., and W.N. Ehmann, Zr-Hf fractionation in chemically defined lunar rock groups, *Proc. Lunar Sci. Conf. 7th*, 3397-3410, 1976.

Goins, N.R., A.M. Dainty, and M.N. Toksöz, Lunar seismology: The internal structure of the Moon, *J. Geophys. Res., 86*, 5061-5074, 1981.

Green, D.H., A.E. Ringwood, W.O. Hibberson, and N.G. Ware, Experimental petrology of Apollo 17 mare basalts, *Proc. Lunar Sci. Conf. 6th*, 871-893, 1975.

Green, T.H., Experimental studies of trace-element partitioning applicable to igneous petrogenesis – Sedona 16 years later, *Chem. Geol., 117*, 1-36, 1994.

Hartmann, W.K., Moon origin: the Impact trigger hypothesis, in *Origin of the Moon,* edited by W.K. Hartmann, R.J. Phillips, and G.J. Taylor, pp. 579-608, Lunar and Planet. Inst., Houston, Tex.,1986.

Hartmann, W.K., and D.R. Davis, Satellite-sized planetesimals and lunar origin, *Icarus, 24*, 504-515, 1975.

Haskin, L.A., J.W. Jacobs, J.C. Brannon, and M.A. Haskin, Compositional dispersions in lunar and terrestrial basalts, *Proc. Lunar Sci. Conf. 8th*, 1731-1750, 1977.

Hess, P.C., The ilmenite liquidus and segregation depths of high-Ti picrite glasses, *Lunar Planet. Sci., XXIV*, 649-650, 1993.

Hess, P.C., Petrogenesis of lunar troctolites, *J. Geophys. Res., 99*, 19,083-19,093, 1994.

Hess, P.C., On the source regions for mare picritic glasses, *J. Geophys. Res., 105*, 4347-4360, 2000.

Hess, P.C., and E.M. Parmentier, A model for the thermal and chemical evolution of the Moon's interior: Implications for the onset of mare volcanism, *Earth Planet. Sci. Lett., 134*, 501-514, 1995.

Hood, L.L., Geophysical constraints on the lunar interior, in *Origin of the Moon,* edited by W.K. Hartmann, R.J. Phillips, and G.J. Taylor, pp. 361-410, Lunar and Planet. Inst., Houston, Tex.,1986.

Hood, L.L., and J.H. Jones, Geophysical constraints on lunar bulk composition and structure: A reassessment, *Proc. Lunar Planet. Sci. Conf. 17th, Part 2, J. Geophys. Res., 92*, suppl., E396-E410, 1987.

Hood, L.L., and M.T. Zuber, Recent refinements in geophysical constraints on lunar origin and evolution, in *Origin of the Earth and Moon*, pp. 397-409, Univ. of Ariz. Press, Tucson, 2000.

Hood, L.L., D.L. Mitchell, R.P. Lin, M.H. Acuna, and A.B. Binder, Initial measurements of the lunar induced magnetic dipole moment using Lunar Prospector magnetometer data, *Geophys. Res. Lett., 26*, 2327-2330, 1999.

Hubbard, N., and J.W. Minear, Petrogenesis in a modestly endowed moon, *Proc. Lunar Sci. Conf. 7th*, 3421-3437, 1976.

Hughes, S.S., and R.A. Schmitt, Zr-Hf-Ta fractionation during lunar evolution, *Proc. Lunar Planet. Sci. Conf. 16th, Part 1,* in *J. Geophys. Res., 90*, D31-D45, 1985.

Hughes, S.S., J.W. Delano, and R.A. Schmitt, Apollo 15 yellow-brown volcanic glass: Chemistry and petrogenetic relations to green volcanic glass and olivine-normative mare basalts, *Geochim. Cosmochim. Acta, 52*, 2379-2391, 1988.

Hughes, S.S., J.W. Delano, and R.A. Schmitt, Petrogenetic modeling of 74220 high-Ti orange volcanic glasses and the Apollo 11 and 17 high-Ti mare basalts, *Proc. Lunar Planet. Sci. Conf. 19th*, 175-188, 1989.

James, O.B., and T.L. Wright, Apollo 11 and 12 mare basalts and gabbros: Classification, compositional variations, and possible petrogenetic relations, *Geol. Soc. Am. Bull., 83*, 2357-2382, 1972.

Jenner, G.A., H.P. Longerich, S.E. Jackson, and B.J. Fryer, ICP-MS: A powerful tool for high-precision trace-element analysis in Earth sciences: Evidence from analysis of selected USGS reference samples, *Chem. Geol., 83*, 133-148, 1990.

Kahn, A., K. Mosegaard, and K.L. Rasmussen, Lunar models obtained from a Monte Carlo inversion of the Apollo seismic P and S waves (CD-ROM abstract #1341), *Lunar Planet. Sci. XXXI*, 2000.

Kesson, S.E., Mare basalts: Melting experiments and petrogenetic interpretations, *Proc. Lunar Sci. Conf. 6th*, 921-944, 1975.

Kesson, S.E., and A.E. Ringwood, Mare basalt petrogenesis in a dynamic Moon, *Earth Planet. Sci. Lett., 30*, 155-163, 1976.

Kuskov, O.L., Constitution of the Moon, 3, composition of the middle mantle from seismic data, *Phys. Earth Planet. Inter., 90*, 55-74, 1995.

Kuskov, O.L., Constitution of the Moon, 4, composition of the mantle from seismic data, *Phys. Earth Planet. Inter, 102*, 239-257, 1997.

Kuskov, O.L., and O.B. Fabrichnaya, Constitution of the Moon, 2, composition and seismic properties of the lower mantle, *Phys. Earth Planet. Inter., 83*, 197-216, 1994.

Kuskov, O.L., and V.A. Kronrod, Constitution of the Moon, 5, constraints on the composition, denisty, temperature, and radius of a core, *Phys. Earth Planet. Inter., 107*, 285-306, 1998.

Lindstrom, M.M., and L.A. Haskin, Compositional inhomogeneities in a single Icelandic tholeiite flow, *Geochim. Cosmochim. Acta, 45*, 15-31, 1981.

Longhi, J., On the connection between mare basalts and picritic volcanic glasses. *Proc. Lunar Planet. Sci. Conf. 17th, Part 2, J. Geophys. Res., 92*, suppl., E349-E360, 1987.

Longhi, J., Differentiates of the picritic glass magmas: The missing mare basalts. In *Workshop on Lunar Volcanic Glasses: Scientific and Resource Potential*, edited by J.W. Delano and G.H. Heiken, pp. 46-47, *LPI Tech. Rep. 90-02*, Lunar and Planet. Inst., Houston, Tex., 1990.

Longhi, J., Experimental petrology and petrogenesis of mare volcanics, *Geochim. Cosmochim. Acta, 56*, 2235-2252, 1992.

Longhi, J., Liquidus equilibria of lunar analogs at high pressure (abstract), *Lunar Planet. Sci., XXIV*, 895-896, 1993.

McCallum, I.S., and M.P. Charette, Zr and Nb partition coefficients: Implications for the genesis of mare basalts, KREEP, and sea floor basalts, *Geochim. Cosmochim. Acta, 42*, 859-869, 1978.

McGinnis, C.E, J.C. Jain, and C.R. Neal, Characterization of memory effects and development of an effective protocol for the measurement of petrogenetically critical trace elements in geological samples by ICP-MS, *Geostand. Newsl., 21*, 289-305, 1997.

McKay, G.A., and D.F. Weill, Petrogenesis of KREEP, *Proc. Lunar Sci. Conf. 7th*, 2427-2447, 1976.

McKay, G.A., and D.F. Weill, KREEP petrogenesis revisited, *Proc. Lunar Sci. Conf. 8th*, 2339-2355, 1977.

McKay, G.A., H. Wiesmann, L.E. Nyquist, J.L. Wooden, and B.M. Bansal, Petrology, chemistry, and chronology of 14078: Chemical constraints on the origin of KREEP, *Proc. Lunar Planet. Sci. Conf. 9th*, 661-687, 1978.

McKay, G.A., H. Wiesmann, B.M. Bansal, and C.-Y. Shih, Petrology, chemistry, and chronology of Apollo 14 KREEP basalts, *Proc. Lunar Planet. Sci. Conf. 10th*, 181-205, 1979.

McKay, G.A., J. Wagstaff, and S.-R. Yang, Zirconium, hafnium, and rare earth element partition coefficients for ilmenite and other minerals in high-Ti lunar mare basalts: An experimental study, *Proc. Lunar Planet. Sci. Conf. 16th, Part 2, J. Geophys. Res. 91*, suppl., D229-D237, 1986.

Morgan, J.W., J.C. Laul, U. Krähenbühl, R. Ganapathy, and E. Anders, Major impacts on the Moon: Characterization from trace elements in Apollo 12 and 14 samples, *Proc. Lunar Sci. Conf. 3rd*, 1377-1395, 1972a.

Morgan, J.W., U. Krähenbühl, R. Ganapathy, and E. Anders, Trace elements in Apollo 15 samples: Implications for meterite influx and volatile depletion on the Moon, *Proc. Lunar Sci Conf. 3rd*, 1361-1376, 1972b.

Morgan, J.W., R. Ganapathy, H. Higuchi, U. Krähenbühl, and E. Anders, Lunar basins: Tentative characterization of projectiles from meteoritic elements in Apollo 17 boulders, *Proc. Lunar Sci. Conf. 5th*, 1703-1736, 1974.

Mueller, S., G.J. Taylor, and R.J. Phillips, Lunar compositions: A geophysical and petrological synthesis, *J. Geophys. Res., 93*, 6338-6352, 1988.

Nakamura, Y., Seismic velocity structure of the lunar mantle, *J. Geophys. Res., 88*, 677-686, 1983.

Nakamura, Y., G.V. Latham, D. Lammlein, M. Ewing, F. Duennebier, and H.J. Dorman, Deep lunar interior inferred from recent seismic data. *Geophys. Res. Lett., 1*, 137-140, 1974.

Neal, C.R., Mare basalts as mantle probes: Dichotomies between Remotely gathered and sample data? (abstract), in *New Views of the Moon: Integrated Remotely Sensed, Geophysical, and Sample Datasets*, pp. 63-64. Lunar and Planet. Inst., Houston, Tex., 1998.

Neal, C.R., The interior of the Moon, core formation, and the Lunar hotspot: What samples tell us (abstract), in *New Views of the Moon II: Understanding the Moon Through the Integration of Diverse Datasets,* pp. 43-44, *LPI Contrib. 980,* Lunar and Planet. Inst., Houston, Tex., 1999.

Neal, C.R., and L.A. Taylor, Petrogenesis of mare basalts: A record of lunar volcanism, *Geochim. Cosmochim. Acta, 56*, 2177-2211, 1992.

Neal, C.R., L.A. Taylor, and M.M. Lindstrom, Apollo 14 mare basalt petrogenesis: Assimilation of KREEP-like components by a fractionating magma, *Proc. Lunar Planet. Sci. Conf. 18th*, 139-153, 1988a.

Neal, C.R., L.A. Taylor, and M.M. Lindstrom, The importance of lunar granite and KREEP in very high potassium (VHK) basalt petrogenesis, *Proc. Lunar Planet. Sci. Conf. 18th*, 121-137, 1988b.

Neal, C.R., L.A. Taylor, R.A. Schmitt, S.S. Hughes, and M.M. Lindstrom, High-alumina (HA) and very high potassium (VHK) basalt clasts from Apollo 14 breccia, part 2, whole rock geochemistry: Further evidence for combined assimilation and fractional crystallization within the lunar crust, *Proc. Lunar Planet. Sci. Conf. 19th*, 147-161, 1989.

Neal, C.R., L.A. Taylor, A.D. Patchen, S.S. Hughes, and R.A. Schmitt, The significance of fractional crystallization in the petrogenesis of Apollo 17 Type A and B high-Ti basalts, *Geochim. Cosmochim. Acta, 54*, 1817-1833, 1990.

Neal, C.R., M.D. Hacker, L.A. Taylor, R.A. Schmitt, and Y.-G. Liu, Basalt generation at the Apollo 12 site, part 2: Source heterogeneity, multiple melts, and crustal contamination, *Meteoritics, 29*, 349-361, 1994.

Ringwood, A.E., and S.E. Kesson, A dynamic model for mare basalt petrogenesis, *Proc. Lunar Sci. Conf. 7th*, 1697-1722, 1976.

Schuraytz, B.C., and G. Ryder, A new petrochemical data base of Apollo 15 olivine-normative mare basalts (abstract), *Lunar Planet. Sci., XIX*, 1041-1042, 1988.

Schuraytz, B.C., and G. Ryder, The contrast of chemical modeling with petrographic reality: Tapping of Apollo 15 olivine-normative mare basalt magma (abstract), *Lunar Planet. Sci., XXII*, 1199-1200, 1991.

Shearer, C.K., and J.J. Papike, Basaltic magmatism on the Moon: A perspective from volcanic picritic glass beads, *Geochim. Cosmochim. Acta, 57*, 4785-4812, 1993.

Shearer, C.K., and J.J. Papike, Magmatic evolution of the Moon, *Am. Mineral., 84*, 1469-1494, 1999.

Shearer, C.K., J.J. Papike, S.B. Simon, K.C. Galbreath, and N. Shimizu, A comparison of picritic glass beads from the Apollo 14 and Apollo 17 sites: Implications for basalt petrogenesis and compositional variability in the lunar mantle (abstract), *Lunar Planet. Sci., XX*, 996-997, 1989.

Shearer, C.K., J.J. Papike, S.B. Simon, K.C. Galbreath, N. Shimizu, Y. Yurimoto, and S. Sueno, Ion microprobe studies of REE and other trace elements in Apollo 14 volcanic glass beads and comparison to Apollo 14 mare basalts, *Geochim. Cosmochim. Acta, 54*, 851-867, 1990.

Shearer, C.K., J.J. Papike, K.C. Galbreath, and N. Shimizu, Exploring the lunar mantle with secondary ion mass spectrometry: A comparison of lunar picritic glass beads from the Apollo 14 and Apollo 17 sites, *Earth Planet. Sci. Lett., 102*, 134-147, 1991.

Shearer, C.K., G.D. Layne, and J.J. Papike, The systematics of light lithophile elements in lunar picritic glasses: Implications for basaltic magmatism on the Moon and the origin of the Moon, *Geochim. Cosmochim. Acta, 58*, 5349-5362, 1994.

Shearer, C.K., J.J. Papike, and G.D. Layne, The role of ilmenite in the source region for mare basalts: Evidence from niobium, zirconium, and cerium in picritic glasses, *Geochim. Cosmochim. Acta, 60*, 3521-3530, 1996a.

Shearer, C.K., J.J. Papike, and G.D. Layne, Deciphering basaltic magmatism on the Moon from compositional variations in the Apollo 15 very low-Ti picritic magmas, *Geochim. Cosmochim. Acta, 60*, 509-528, 1996b.

Shervais, J.W., L.A. Taylor, J.C. Laul, C.-Y. Shih, and L.E. Nyquist, Very high potassium (VHK) basalts: Complications in mare basalt petrogenesis, *Proc. Lunar Planet. Sci. Conf. 16th, Part 1, J. Geophys. Res., 90*, suppl., D3-D18, 1985a.

Shervais, J.W., L.A. Taylor, and M.M. Lindstrom, Apollo 14 mare basalts: Petrology and geochemistry of clasts from consortium breccia 14321. *Proc. Lunar Planet. Sci. Conf. 15th, Part 2, J. Geophys. Res., 90*, suppl., C375-C390, 1985b.

Shirley, D., and J.T. Wasson, Mechanism for the extrusion of KREEP, *Proc. Lunar Planet. Sci. Conf. 12th*, 965-978, 1981.

Smith, J.V., A.T. Anderson, R.C. Newton, E.J. Olsen, P.J. Wyllie, A.V. Crewe, M.S. Isaacson, and D. Johnson, Petrologic history of the Moon inferred from petrography, mineralogy, and petrogenesis of Apollo 11 rocks, *Proc. Apollo 11 Lunar Sci. Conf.*, 897-925, 1970.

Snyder, G.A., L.A. Taylor, and C.R. Neal, A chemical model for generating the sources of mare basalts: Imperfect, geologically realistic fractional crystallization of the lunar magmasphere, *Geochim. Cosmochim. Acta, 56*, 3809-3823, 1992.

Spera, F.J., Lunar magma transport phenomena, *Geochim. Cosmochim. Acta, 56*, 2253-2265, 1992.

Steele, A.M., R.O. Colson, R.L. Korotev, and L.A. Haskin, Apollo 15 green glass: Compositional distribution and petrogenesis, *Geochim. Cosmochim. Acta, 56*, 4075-4090, 1992.

Sun, S.-S., and W.F. McDonough, Chemical and isotopic systematics of oceanic basalts: Implications for mantle composition and processes. In *Magmatism in the Ocean Basins*. Edited by A.D. Saunders and M.J. Norry, *Geol. Soc. Spec. Publ. 42*, 313-345, 1989.

Tatsumoto, M., R.J. Knight, and C.J. Allegre, Time differences in the formation of meteorites as determined from the ratio of lead-207 to lead-206, *Science, 180*, 1279-1283, 1973.

Tatsumoto, M., W.R. Premo, and D.M. Unruh, Origin of lead from green glass of Apollo 15426: A search for primitive lunar lead, *Proc. Lunar Planet. Sci. Conf. 17th, Part 2, J. Geophys. Res., 92*, suppl., E361-E371, 1987.

Taylor, G.J., R.D. Warner, and K. Keil, VLT mare basalts: Impact mixing, parent magma types, and petrogenesis, in *Mare Crisium: The View From Luna 24*, edited by R.B. Merrill and J.J. Papike, pp. 357-370, Pergamon Press, New York, 1978.

Taylor, S.R., *Planetary Science: A Lunar Perspective*, 481 pp., Lunar and Planet. Inst., Houston, Tex., 1982.

Taylor, S.R., *Solar System Evolution: A New Perspective,* 307 pp., Cambridge Univ. Press, New York, 1990.

Taylor, S.R., and P. Jâkes, The geochemical evolution of the Moon, *Proc. Lunar Sci. Conf. 5th*, 1287-1305, 1974.

Vaniman, D.T., and J.J. Papike, Very low-Ti (VLT) basalts: A new mare rock type from the Apollo 17 drill core, *Proc. Lunar Sci. Conf. 8th*, 1443-1471, 1977.

Vaniman, D.T. and J.J. Papike, Lunar highland melt rocks: Chemistry, petrology, and silicate mineral chemistry, *Proceedings of the Conference on the Lunar Highlands Crust*, edited by J.J. Papike and R.B. Merril, pp. 271-337, Pergamon, New York, 1980.

Vetter, S.K., J.W. Shervais, and M.M. Lindstrom, Petrology and geochemistry of olivine-normative and quartz-normative basalts from regolith breccia 15498: New diversity in Apollo 15 mare basalts, *Proc. Lunar Planet. Sci. Conf. 18th*, 255-271, 1988.

Wagner, T.P., and T.L. Grove, Origin of high-Ti lunar ultramafic glasses (abstract), *Lunar Planet. Sci., XXIV*, 1475-1476, 1993.

Wagner, T.P., and T.L. Grove, Origin of high-Ti lunar magma by erosion of ilmenite (abstract), *Lunar Planet. Sci., XXVI*, 1455-1456, 1995.

Wagner, T.P., and T.L. Grove, Experimental constraints on the origin of lunar high-Ti ultramafic glasses, *Geochim. Cosmochim. Acta, 61*, 1315-1327, 1997.

Walker, D., J. Longhi, E.M. Stolper, T.L. Grove, and J.F. Hays, Origin of titaniferous basalts, *Geochim. Cosmochim. Acta, 39*, 1219-1235, 1975.

Walker, D., J. Longhi, R.J. Kirkpatrick, and J.F. Hays, Differentiation of an Apollo 12 picrite magma, *Proc. Lunar Sci. Conf. 7th*, 1365-1389, 1976.

Warner, R.D., G.J. Taylor, G.H. Conrad, H.R. Northrop, S. Barker, K. Keil, M.-S. Ma, and R.A. Schmitt, Apollo 17 high-Ti mare basalts: New bulk compositional data, magma types, and petrogenesis, *Proc. Lunar Planet. Sci. Conf. 10th*, 225-227, 1979.

Warner, R.D., G.J. Taylor, K. Keil, M.-S. Ma, and R.A. Schmitt, Aluminous mare basalts: New data from Apollo 14 coarse-fines, *Proc. Lunar Planet. Sci. Conf. 11th*, 87-104, 1980.

Warren, P.H., The magma ocean concept and lunar evolution. *Annu. Rev. Earth Planet. Sci., 13*, 201-240, 1985.

Warren, P.H., and J.T. Wasson, The origin of KREEP, *Rev. Geophys., 17*, 73-88, 1979.

Wood, J.A., J.S. Dickey Jr., U.B. Marvin, and B.N. Powell, Lunar anorthosites and a geophysical model of the Moon, *Proc. Apollo 11 Lunar Sci. Conf.*, 965-988, 1970.

C. R. Neal, Department of Civil Engineering and Geological Sciences, University of Notre Dame, Notre Dame, IN 46556-0767, USA. (neal.1@nd.edu)

(Received September 15, 2000; revised April 11, 2001; accepted May 30, 2001.)